Electronic Supplementary Material (ESI) for Journal of Materials Chemistry A.

SUPPORTING INFORMATION

Insights into Dual-Functional Modification for Water Stability Enhancement of Mesoporous Zirconium Metal–Organic Frameworks

Jian Liu,[*,a] Ryther Anderson,[b] Kevin M. Schmalbach,[c] Thomas R. Sheridan,[a] Zhao Wang,[d] Neil M. Schweitzer,[e] Andreas Stein,[d] Nathan A. Mara,[c] Diego Gomez-Gualdron,[b] and Joseph T. Hupp[*,a]

[a] Department of Chemistry, Northwestern University, 2145 Sheridan Road, Evanston, Illinois 60208, United States
[b] Department of Chemical and Biological Engineering, Colorado School of Mines, Golden, Colorado 80401, United States
[c] Department of Chemical Engineering and Materials Science, University of Minnesota, Minneapolis, Minnesota 55455, United States
[d] Department of Chemistry, University of Minnesota, 207 Pleasant Street SE, Minneapolis, Minnesota 55455, United States
[e] Department of Chemical and Biological Engineering, Northwestern University, 2145 Sheridan Road, Evanston, Illinois 60208, United States

Corresponding Authors: Jian Liu, jian.liu@northwestern.edu; Joseph T. Hupp, j-hupp@northwestern.edu.

Table of Contents

List of Figures

Materials

Zirconyl chloride octahydrate, 1,3,6,8-tetrabromopyrene, (4-(methoxycarbonyl)phenyl)-boronic acid, K_3PO_4, tetrakis(triphenylphosphine) palladium (0), trifluoroacetic acid, hydrochloric acid, benzoic acid, 1,3-bis(trifluoromethyl)-5-bromobenzene, acetylacetone (HAcac), hexafluoroacetylacetone (HFacac), and 1,1,1-trifluoroacetylacetone (HTFacac) were purchased from Sigma Aldrich Chemicals Company, Inc. (Milwaukee, WI) and were used as received. The NU-1000 ligand, 1,3,6,8-tetrakis(*p*-benzoic acid)pyrene (H_4TBAPy), was synthesized based on our previous procedures.[1] Concentrated sulfuric acid was purchased from VWR Scientific, LLC (Chicago, IL). Acetone, chloroform, 1,4-dioxane, tetrahydrofuran, heptane, and *N*,*N*-dimethylformamide (DMF) were obtained from Sigma Aldrich and used without further purification. Deuterated dimethylsulfoxide (d_6-DMSO), deuterated chloroform-d ($CDCl_3$), deuterated sulfuric acid D_2SO_4 (d_2) (96-98% solution in D_2O), deuterium oxide, and sodium deuteroxide solution (40 wt. % in D_2O, 99.5 atom% D) were obtained from Cambridge Isotope Laboratory. All gases used for the adsorption and desorption measurements were Ultra High Purity Grade 5 and were obtained from Airgas Specialty Gases (Chicago, IL).

Experimental

Synthesis of NU-1000-F. $ZrOCl_2 \cdot 8H_2O$ (98 mg, 0.30 mmol) and benzoic acid (2 g, 16.38 mmol) were ultrasonically dissolved in an 8-dram glass vial containing 8 mL of DMF. The mixture was transferred to an oven at 100 °C to incubate for 1 h. H_4TBAPy (40 mg, 0.06 mmol) and TFA (40 µL, 0.52 mmol) were added together into the prepared solution at room temperature. Sonicated the yellow suspension for 10 min and placed in a pre-heated oven at 100 °C for 18 h. The yellow product was isolated by centrifuging for 10 min at 8000 rpm. It was washed for three times using 15 mL DMF each time and soaking 1 h between washes. Coordinated modulators in the as-synthesized yellow powder were removed by washing using 0.6 mL of 8 M aqueous HCl in 15 mL DMF at 100 °C overnight. The resulting powder was isolated by centrifugation and washed with 15 mL DMF and acetone three times, respectively. The final product was isolated by centrifugation and dried in a vacuum oven at 80 °C for 1 h followed by further activation at 120 °C using a Micromeritics Smart VacPrep instrument.

Synthesis of NU-1000-FF. As-synthesized NU-1000-F (50 mg, 0.023 mmol) was suspended in 15 mL 1,4-dioxane. 0.6 mL 8M aqueous HCl was added into NU-1000-F solution and was kept at room temperature overnight. The yellow powder was isolated by centrifugation and washed using 1,4-dioxane followed by solvent-exchanging with ethanol using 10 mL ethanol for three times. 4 equivalents (11.2 µL, 0.08 mmol) of triethylamine (TEA) were added into 10 mL ethanol mixture and kept at room temperature overnight. TEA treatment was repeated again to completely remove the chlorine anions. The resulting powder was isolated by centrifugation and solvent-exchanged using acetone for three times. The final product was isolated by centrifugation and dried in a vacuum oven at 80 °C for 2 h followed by further activation at 120 °C using a Micromeritics Smart VacPrep instrument.

Synthesis of Acac/TFacac/Facac-NU-1000. As-synthesized NU-1000-F (50 mg, 0.023 mmol) was suspended in 10 mL anhydrous heptane. Eight equivalents (0.2 mmol) of

acetylacetone (1,1,1-trifluoroacetylacetone or hexafluoroacetylacetone) were added into the NU-1000-F solution, which was then kept at room temperature overnight. The yellow product was isolated by centrifugation for 10 min at 8000 rpm. It was washed three times using 10 mL heptane and soaking for 1 h between washes. The resulting powder was isolated by centrifugation and washed with 15 mL acetone for three times. The final product was isolated by centrifugation and dried in a vacuum oven at 80 °C for 2 h followed by further activation at 120 °C using a Micromeritics Smart VacPrep instrument.

Characterization Methods

^{1}H-NMR (Base Digestion). NMR spectra were recorded on a Bruker Avance DPX-500 NMR spectrometer (500 MHz; 64 scans). Chemical shifts were reported in ppm with the residual solvent resonances as the reference. Samples (~ 1 mg) were dissolved in ~ 2 to 3 drops of 0.1 M NaOD/D_2O, sonicated for 30 min until a clear solution was obtained, and further diluted with ~ 25 drops of D_2O. The mixture was centrifuged to separate the yellow solution and the white solid. The upper clear solution was transferred into an NMR tube for measurement.

^{1}H-NMR and ^{19}F-NMR (Acid Digestion). ^{1}H-NMR and ^{19}F-NMR spectra were recorded on a Bruker F500-NMR spectrometer, where the Agilent DD2 500 MHz system has three RF channels. Chemical shifts are reported in ppm with the residual solvent resonances as the reference. Samples (~1 mg) were dissolved in ~2–3 drops of concentrated D_2SO_4 and then diluted with ~30 drops of DMSO-d_6. In order to improve the solubility of TFacac and Facac in DMSO, ~ 5 drops of chloroform-d were added into the dissolved solution of TFacac/Facac-NU-1000 samples. To quantitatively calculate the ratio of TFacac or Facac per Zr_6 node, 5 μL of 1 vol% of 1,3-bis(trifluoromethyl)-5-bromobenzene was added as an internal standard before the analysis.

Diffuse Reflectance Infrared Fourier Transform Spectroscopy (DRIFTS). Spectra were recorded on a Nicolet 6700 FTIR spectrometer equipped with an MCT detector and a Harrick praying mantis accessory. The samples were thermally activated at 120 °C using a Micromeritics Smart VacPrep instrument overnight before each measurement. The spectra were collected at 1 cm^{-1} resolution over 64 scans. A sample of solid KBr was used as the background.

X-ray Photoelectron Spectroscopy (XPS). Measurements were carried out on a Thermo Scientific ESCALAB 250 Xi (Al Kα radiation, hv = 1486.6 eV) equipped with an electron flood gun. XPS data was analyzed using Thermo Scientific Avantage Data System software, and all spectra were referenced to the adventitious C1s peak (284.8 eV).

N_2 Adsorption and Desorption Isotherms. N_2 adsorption and desorption isotherms were measured on a Micromeritics Tristar II 3020 instrument at 77 K. Pore-size distributions were obtained from DFT calculations using a carbon slit-pore model with a N_2 kernel. Before each run, samples were thermally treated at 120 °C for 12 hrs under high vacuum on a Smart VacPrep from Micromeritics.

Scanning Electron Microscopy (SEM). SEM images were collected on a Hitachi SU8030 FE-SEM microscope. Samples were coated with OsO_4 to ~ 9 nm thickness in a Denton Desk III TSC Sputter Coater before imaging.

Water Adsorption-Desorption Isotherms. Water vapor isotherms were measured on a Micromeritics 3Flex in the Reactor Engineering and Catalyst Testing (REACT) core facility at Northwestern University. The water uptake in g/g units is calculated as (adsorbed amount of water)/(amount of adsorbent). Prior to the adsorption measurements, MOFs were thermally treated at temperature of 120 ˚C for 6 hrs under high vacuum on a Micromeritics Smart VacPrep. Prior to the water adsorption measurements, liquid water (analyte) was flash frozen under liquid nitrogen and then evacuated under dynamic vacuum at least 3 times to remove any gases in the water reservoir. The sample temperature was controlled with a Micromeritics ISO controller. Isotherms were collected at specific relative pressures using a 10 second equilibration window.

Mechanical Studies. As previously reported for mechanical studies of NU-1000 particles,[2] a spatula tip of particles of each NU-1000 variant was dispersed in a small amount (~2 mL) of acetone and sonicated for 10 min. A drop of the dispersion was applied to a silicon wafer piece and allowed to dry before attaching the wafer piece to an SEM stub using cyanoacrylate as an adhesive. The mounted samples were stored under vacuum before being quickly transferred to the SEM chamber for mechanical testing, minimizing exposure to moisture. Individual particles were compressed using a Bruker Hysitron PI88 *in situ* nanoindenter equipped with an xR high load transducer and 20 μm diameter diamond flat punch probe operated in a FEI Quanta 200 3D FIB/SEM at 10 kV. A minimum of 4 particles of each variant was compressed in displacement control mode at a rate of 15 nm/s. Finite element modeling of compression along the flat face of the hexagonal cross-section was performed using Abaqus/Standard. In contrast to the previous work, all particles were modeled as dense, isotropic hexagonal prisms with a height of the hexagonal face edge length of 1.25 μm and a length of 8 μm rather than two-dimensional hexagonal cross-sections. R3D4 rigid 3D quadrilateral nodes were used. To correlate initial measured stiffness (slope of load–displacement curve) to effective elastic modulus, a calibration curve was constructed by using an input elastic modulus and measuring the resulting stiffness. After elastic properties were determined, the input elastic modulus was fixed, and a second calibration curve was constructed by using an input isotropic yield stress and measuring the resulting failure load.

Computational Methods. A cluster model of each version of the NU-1000 node was built in Materials Studio, capping the carboxylate groups with $–CH_3$ moieties. Then, the model geometry was optimized in Gaussian16 using density functional theory DFT)) The B3LYP functional was used with non-metal atoms described by the 6-31G* basis set for non-metals and LANL2DZ for Zr (along with the LANL2DZ pseudopotential). Atomic charges were calculated using the CHelpG method with the atomic radii taken from the Universal Force Field (UFF). Each node model with its charge information was used as input for our in-house code Topologically Based Crystal Constructor (ToBaCCo)[3] to build each version of the NU-1000 MOF. This formalism correspond to our previously described Molecular Building Block Based (MBBB) charge assignment method.[4] The built models had their

geometries optimized using molecular mechanics in LAMMPS with interactions described by the UFF4MOF forcefield. The pore volume for each version of NU-1000 was calculated using grand canonical Monte Carlo (GCMC) simulations of N_2 adsorption at 77 K and 1 atm of pressure. The GCMC simulations were done using RASPA treating the MOF as rigid.[5] MOF-N_2 interactions were modeled using a Lennard-Jones (LJ) potential, whereas N_2–N_2 interactions were modeled using LJ and Coulomb interactions. LJ parameters for MOF atoms corresponded to the UFF4MOF, and N_2 parameters corresponded to the TraPPE model. The calculated pore volume was used to estimate the maximum loading of water that each MOF could hold assuming water residing in the pores at liquid density, and then subsequently loading each version of NU-1000 with water at 0, 25, 50, 75, and 100% of the maximum loading.

MD Simulations. Molecular dynamics (MD) simulations were conducted using LAMMPS considering the MOF as flexible. Bonded interactions between MOF atoms were modelled according to UFF4MOF. MOF-MOF, MOF-water and water-water interactions were modelled with LJ + Coulomb potentials, albeit excluding short-range 1-4 Coulomb interactions between MOF atoms. MOF LJ parameters were also obtained from UFF4MOF while MOF charges corresponded to the MBBB method.[4] Water LJ parameters and charges corresponded to the TIP4P/2005 model. Long-range Coulomb interactions were ccalculated according to the particle-particle particle-mesh (PPPM) method with a 12.5 Å cutoff. A 12.5 Å cutoff was also used for all LJ interactions, but analytical tail corrections were performed. The SHAKE algorithm was used to maintain the water molecules rigid in consistency with the TIP4P model. For all MD simulations, we used a 1 fs timestep and a Nosé-Hoover thermostat with a 100 timestep damping parameter. For simulations in the NPT ensemble, we additionally used a Nosé-Hoover barostat with a 1000 timestep damping parameter. All simulations were run at a temperature of 300 K. For each unique structure (i.e., each NU-1000 version and water loading % combination) the lattice constants were calculated based on the average unit cell dimensions during NPT simulations at zero hydrostatic pressure. The average was calculated collecting dimenions every 10 timesteps for 500 ps (after 500 ps of equilibration) . Elastic tensors were calculated using these averaged lattice constants as the reference equilibrium (non-deformed) system, and then applying 12 deformations (forward and backward in six directions) of 1.5% relative to the MOF equilibrium unit cell parameters as in previous work.[3] However, rather than calculating stress for each deformed structure using a zero K energy minimizations, the stresses were calculated as ensemble averages at the deformed lattice parameters and at a finite temperature. Averages were calculated by collecting stresses every 10 timesteps for 50 ps after 50 ps of equilibration. All reported mechanical properties were averaged from ten independent simulations. The radial distribution functions (RDFs) were calculated from short NPT simulations at zero hydrostatic pressure every 10 timesteps for 500 ps (after 500 ps of equilibration) and then averaged.

Dehydration free energies were calculated using the finite-differences thermodynamic integration (FDTI) method described by Mezei.[6] In thermodynamic integration the free energy difference between and initial and final state (whose total energies are U_I and U_F, respectively) is calculated by alchemically switching a system from one state to another

with the aid of a coupling parameter λ. Typically, $\lambda = 0$ in the initial state and $\lambda = 1$ in the final state. The λ-dependent total energy of the system is then

$$U(\lambda) = (1 - \lambda)U_I(\lambda) + \lambda U_F(\lambda) \qquad (1)$$

The free energy difference between the initial and final state can then be calculated as

$$\Delta F = \int_0^1 \left\langle \frac{\partial U(\lambda)}{\partial \lambda} \right\rangle_\lambda d\lambda \qquad (2)$$

where the angled brackets indicate an ensemble average at a specific value of λ. In FDTI, the integrand of Eqn. 2 is estimated at each value of a series of λ values using finite differences. FDTI is discussed in greater detail in ref. 59. In the work here, we switched $\lambda = 1$, for the MOF and 100% water system (i.e., all interactions are present), to $\lambda = 0$, for the empty MOF and isolated water molecules (i.e., the MOF does not interact with any water and the water molecules do not interact with each other), in the NPT ensemble (pressure = 1 atm) in increments of 0.05 with a perturbation of 0.001. That is, λ was perturbed by 0.001 to numerically evaluate the integrand in Eqn. 2 at each value of λ. Water charges were directly scaled by λ to ensure correct evaluation of long-range electrostatics. Soft-core LJ and Coulomb potentials were used for all water interactions, which ensured that no singularities in the integrand of Eqn. 2 were observed due to high energies from atom overlap at intermediate values of λ. Soft-core potentials are identical to the typical functional forms at $\lambda = 1$ and are zero at $\lambda = 0$. However, for intermediate values of λ they yield finite (and relatively low) energies at zero separation distance, so atom overlaps do not result in extremely high energies. The integrand of Eqn. 2 was averaged over 100 ps after 100 ps of equilibration for each value of λ.

Catalytic Hydrolysis Measurements. Hydrolysis profiles were recorded by *in-situ* ^{31}P NMR measurement at 25 °C. The catalysts (6 mol%, 1.5 μmol Zr_6) were added in a 1.5-dram vial, and 1.05 mL of 0.4 M N-ethylmorpholine solution (0.05 mL N-ethylmorpholine, 0.9 mL DI water and 0.1 mL D_2O) was loaded into the vial and then sonicated for 1 min to disperse the MOF powder. After an overnight soaking, 4 μL of DMNP (25 μmol) was added and swirled for 15 s. The reaction mixture was then transferred to an NMR tube and the spectra were instantly recorded; the first data point was collected ~2–3 min after the beginning of the reaction. The progress of the reaction was monitored with 1 min increments for 1 h (number of scans = 16, delay time = 28 s).

Figures

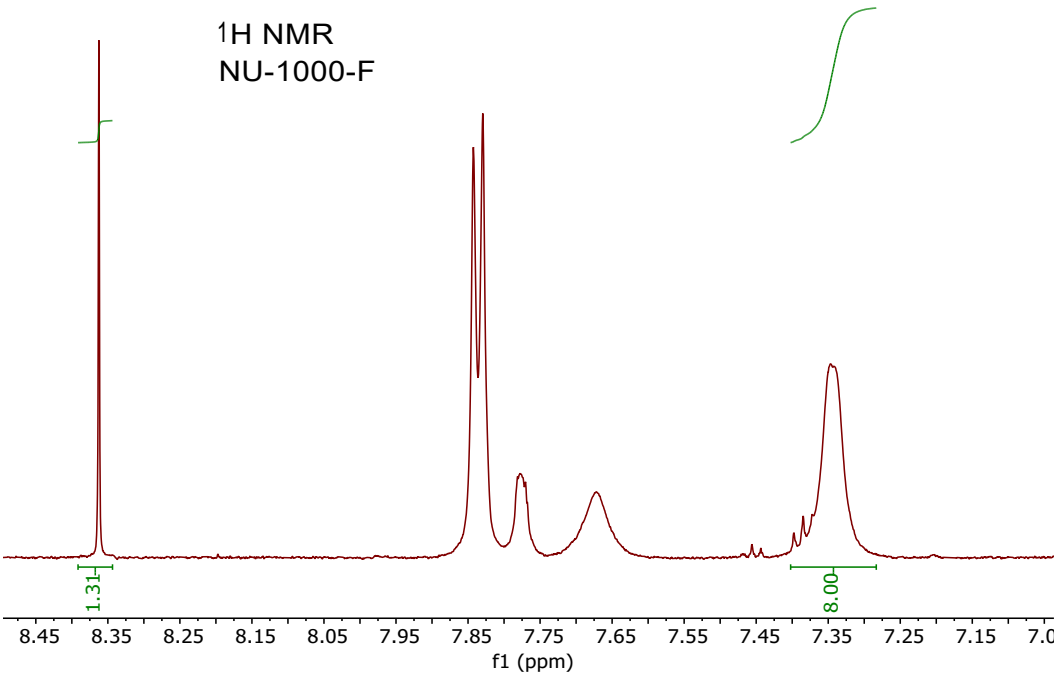

Figure S1. ^{1}H NMR (base digestion) of NU-1000-F.

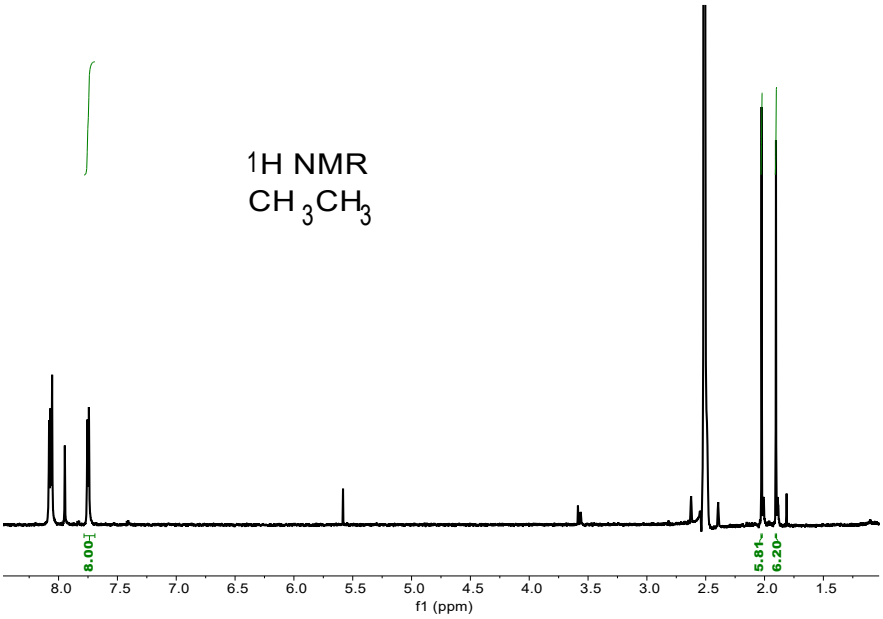

Figure S2. ^{1}H NMR (acid digestion) of Acac-NU-1000.

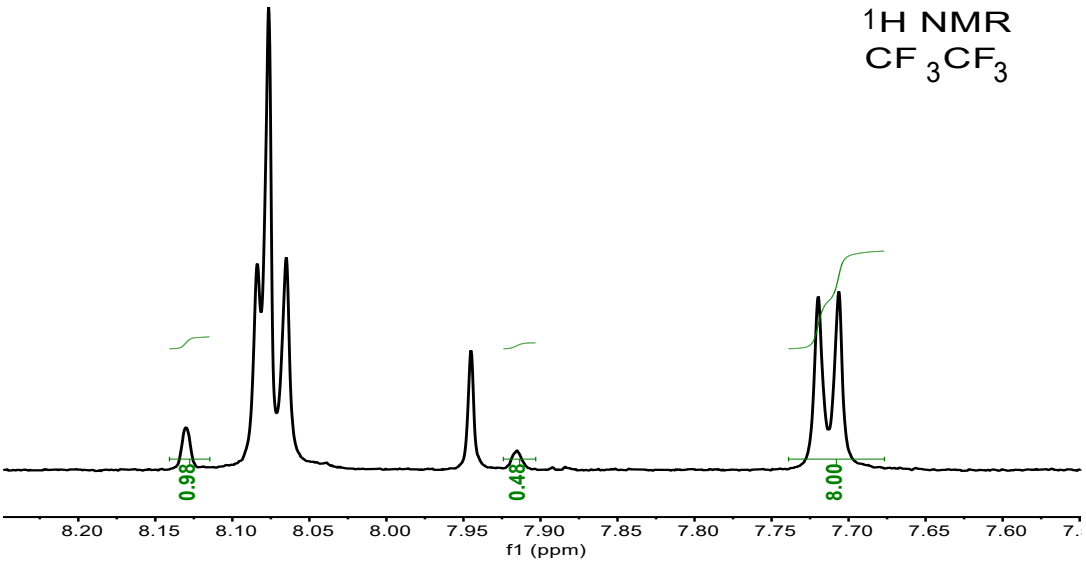

Figure S3. ^{1}H-NMR (acid digestion) of Facac-NU-1000.

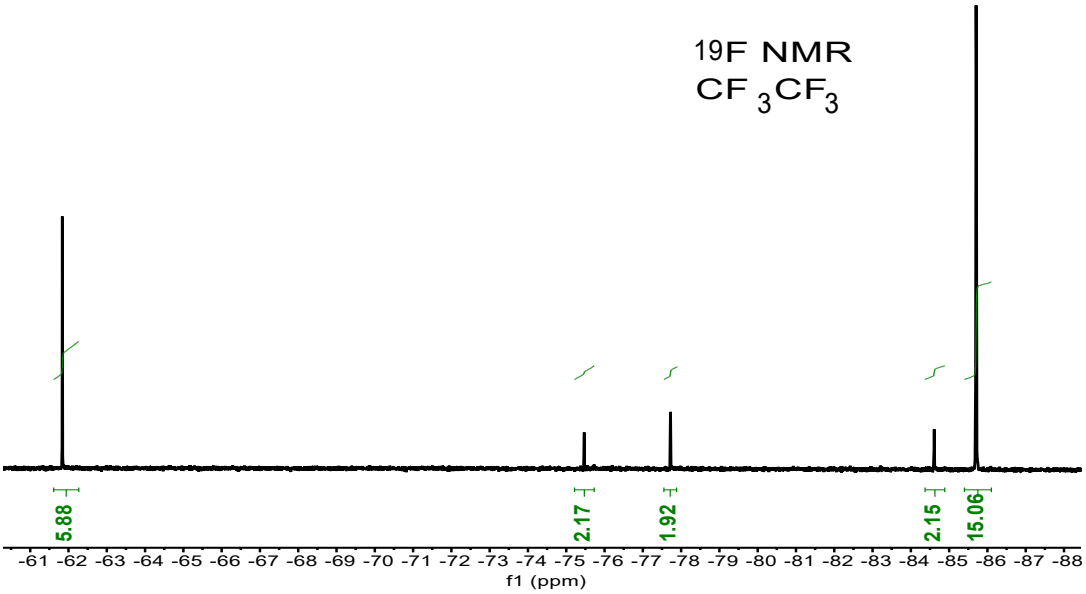

Figure S4. ^{19}F-NMR (acid digestion) of Facac-NU-1000.

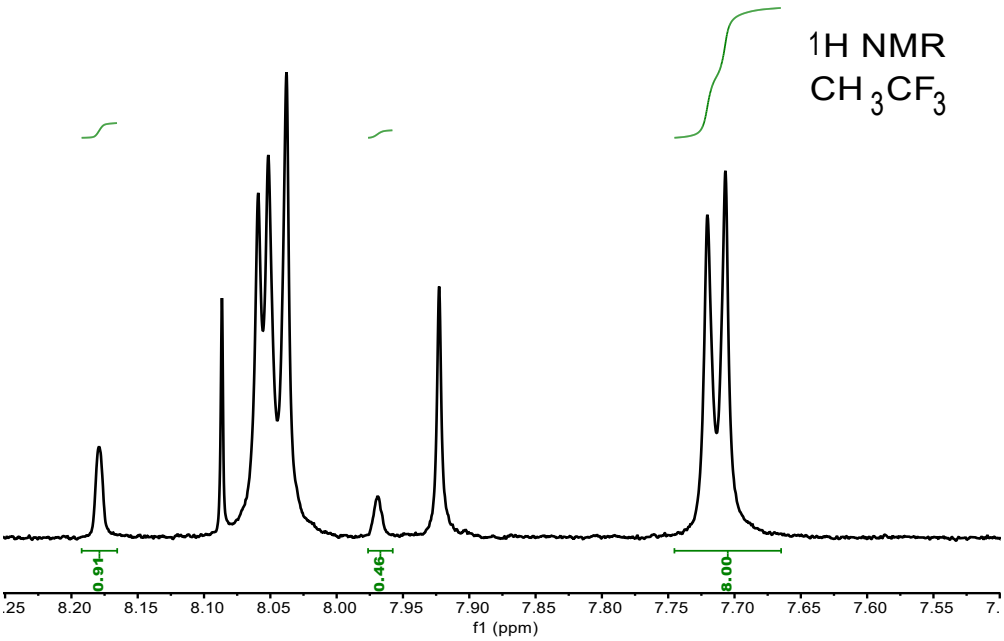

Figure S5. ^{1}H-NMR (acid digestion) of TFacac-NU-1000.

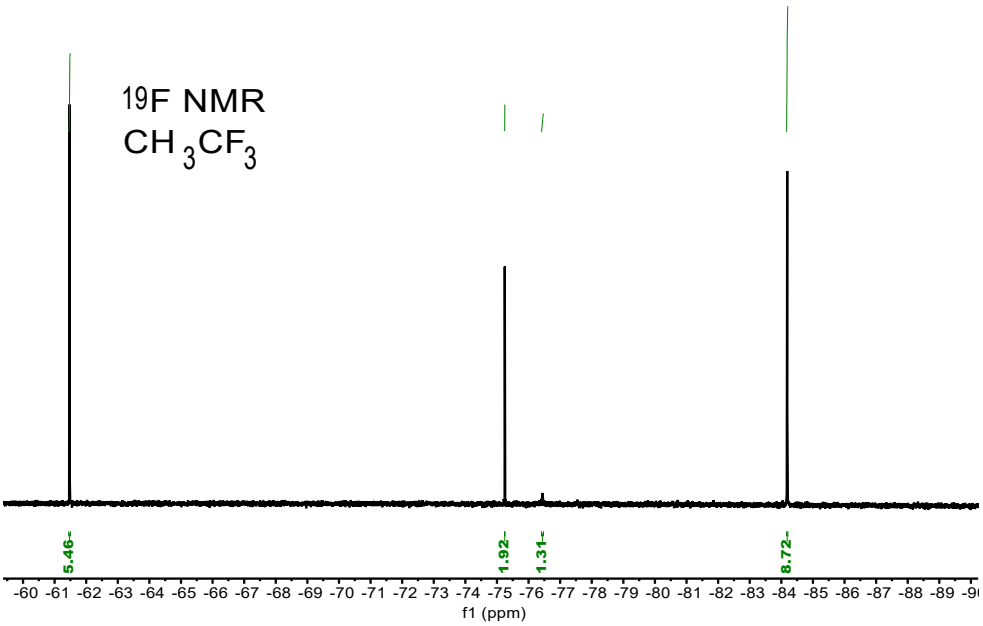

Figure S6. ^{19}F-NMR (acid digestion) of TFacac-NU-1000.

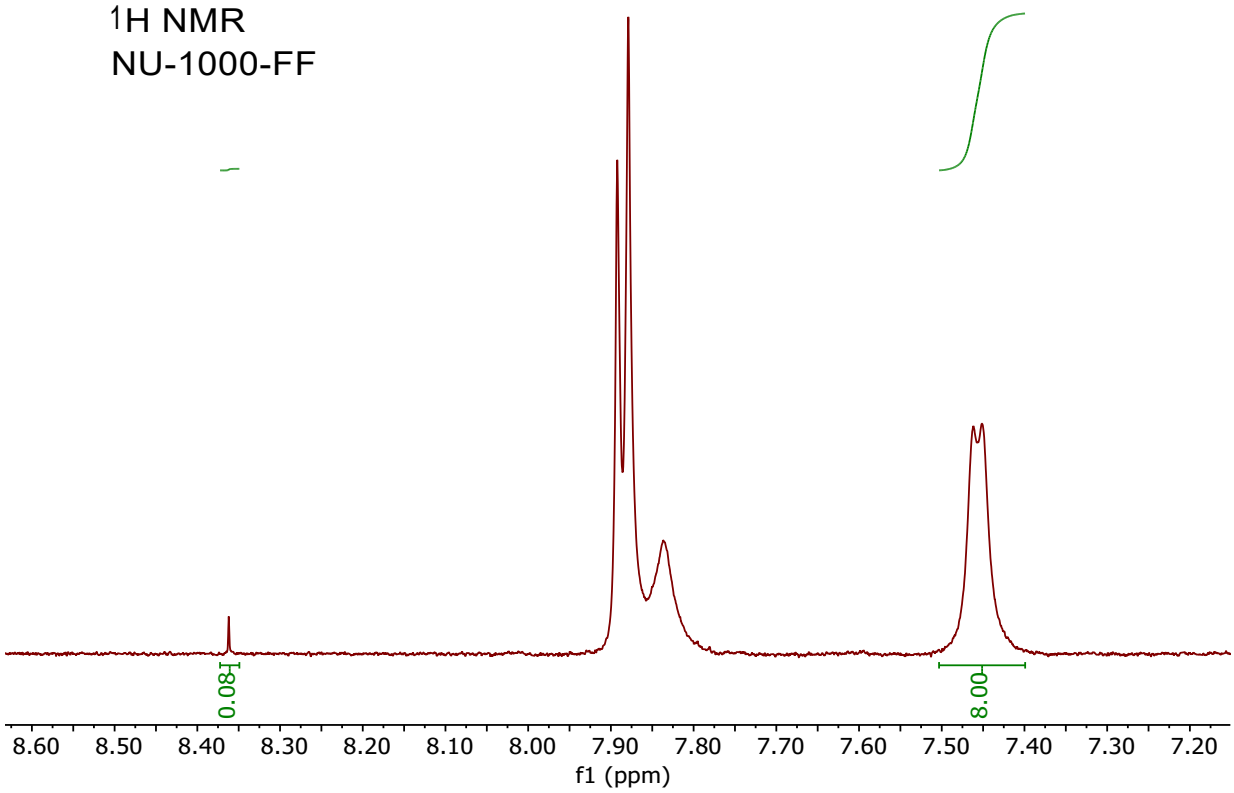

Figure S7. ^{1}H-NMR (base digestion) of as-synthesized NU-1000-FF, showing residual 0.16 formate in the material.

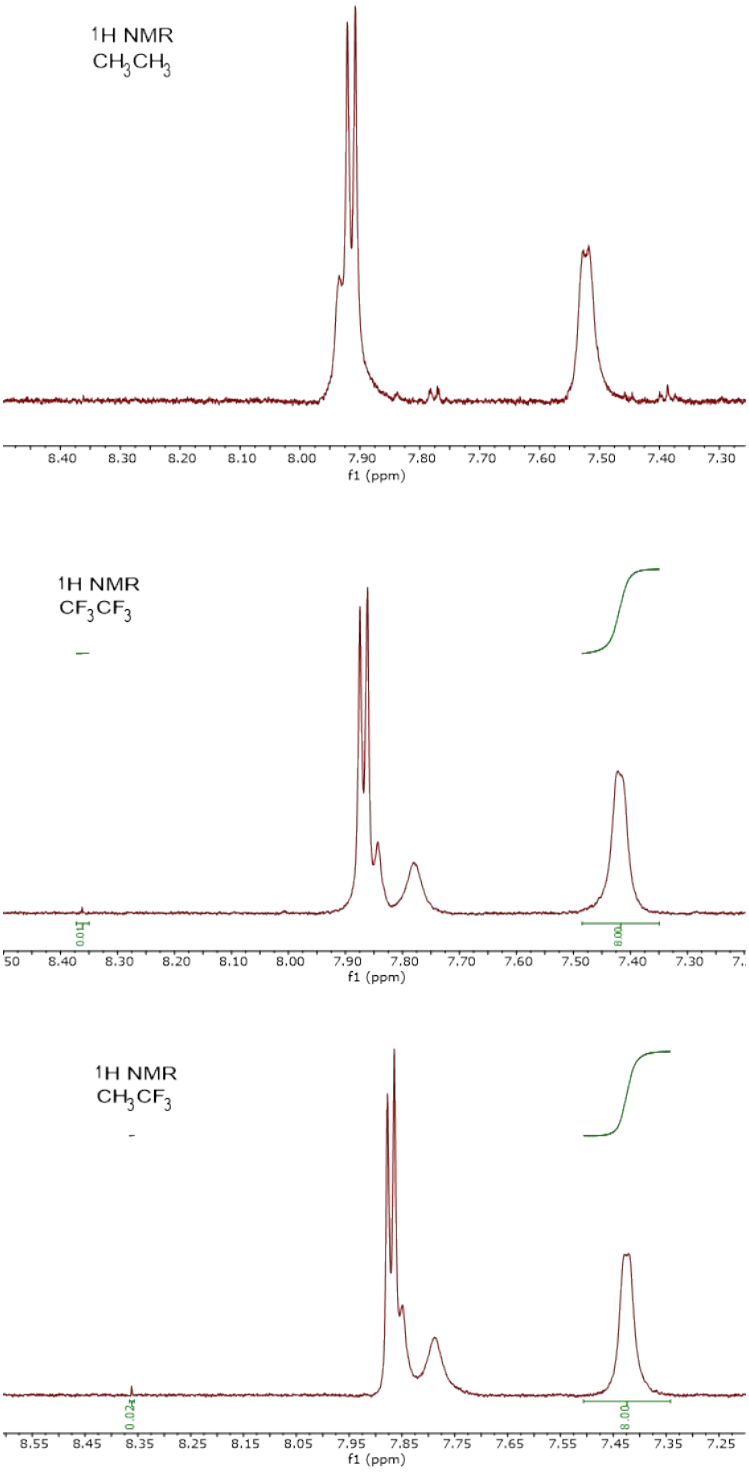

Figure S8. ^{1}H-NMR (base digestion) of Acac-NU-1000, Facac-NU-1000 and TFacac-NU-1000.

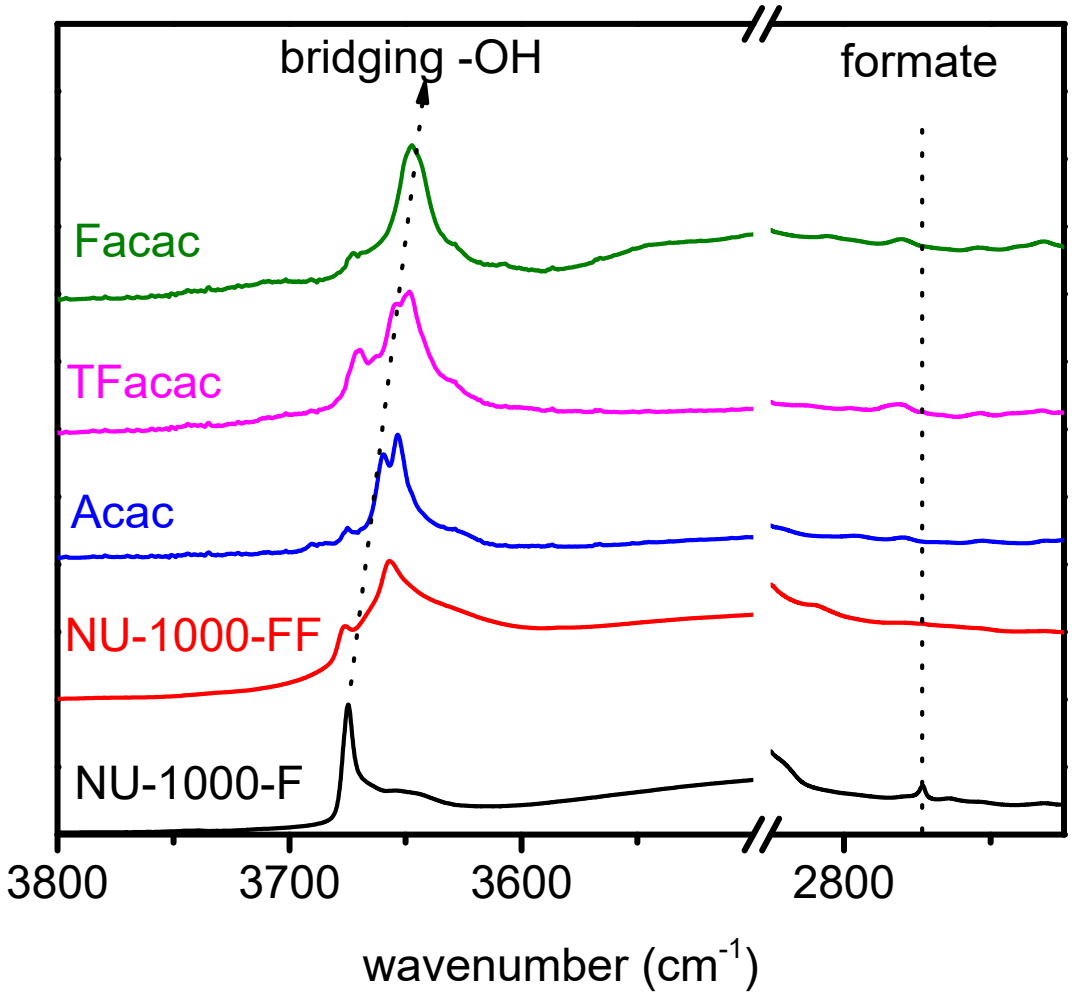

Figure S9. DRIFT spectra of as-synthesized NU-1000-F, NU-1000-FF, Acac-NU-1000, TFacac-NU-1000, and Facac-NU-1000.

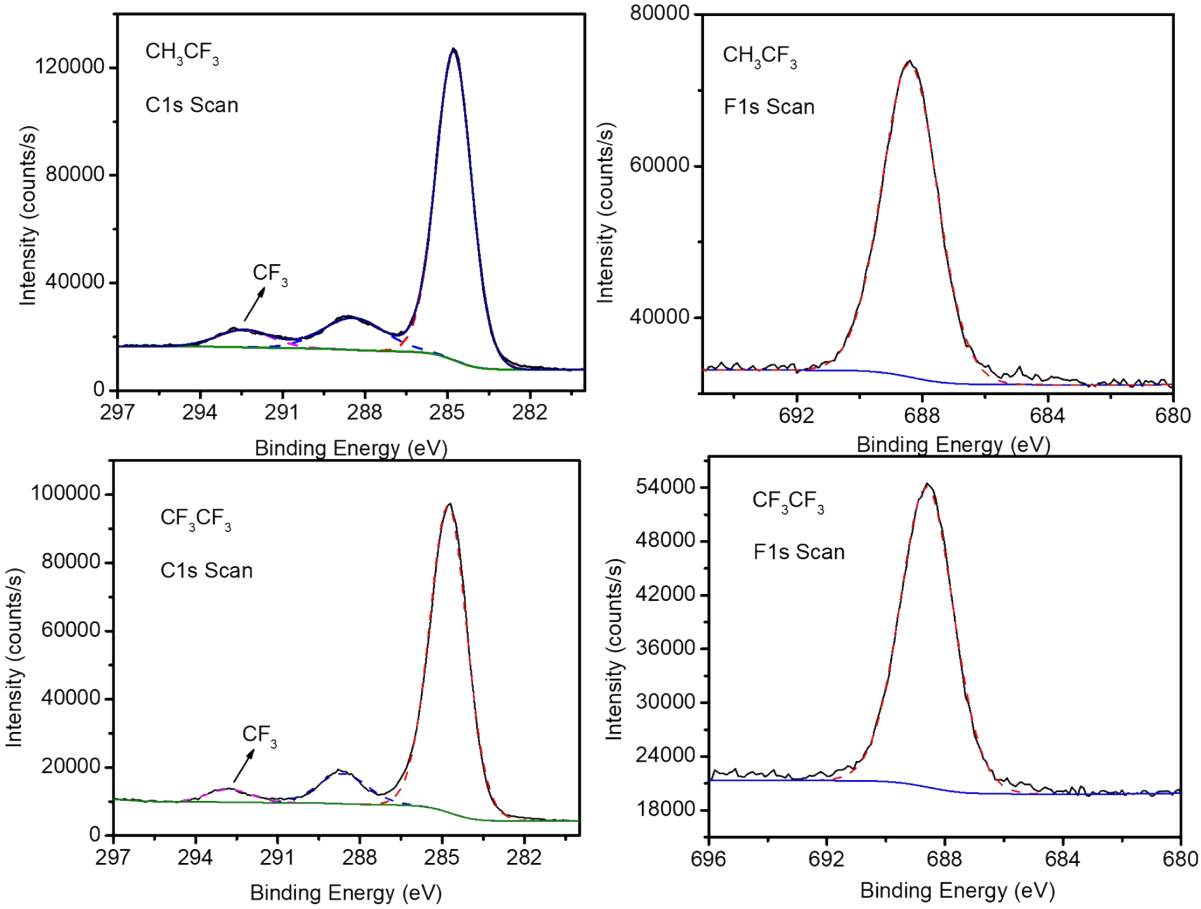

Figure S10. XPS spectra of C1s scan and F1s scan of as-synthesized TFacac-NU-1000 and Facac-NU-1000.

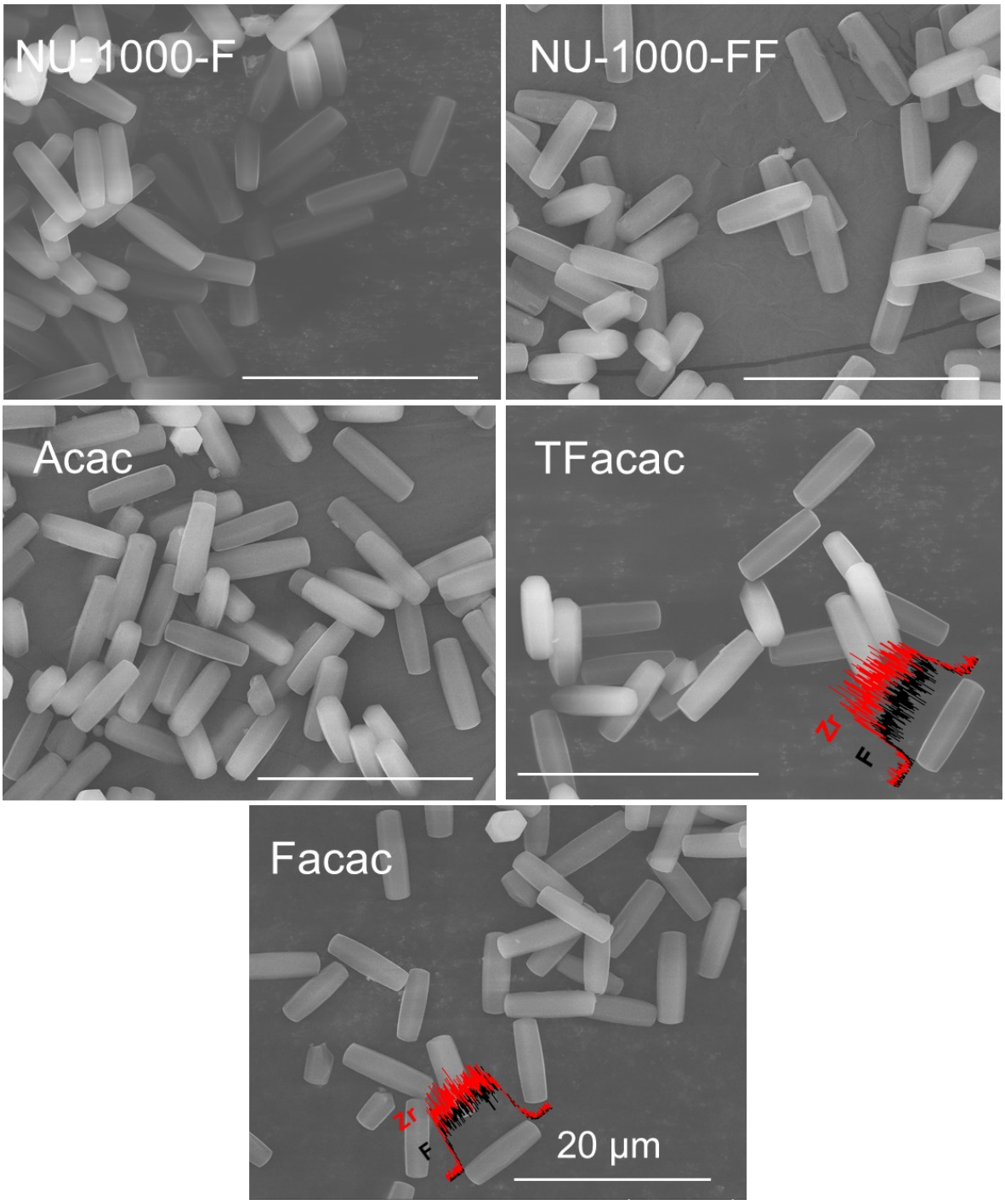

Figure S11. SEM image of NU-1000-F, NU-1000-FF, Acac-NU-1000, TFacac-NU-1000, and Facac-NU-1000 with Zr and F EDS line scans, showing uniform distribution of F throughout the crystals. The scale bar in each image is 20 μm.

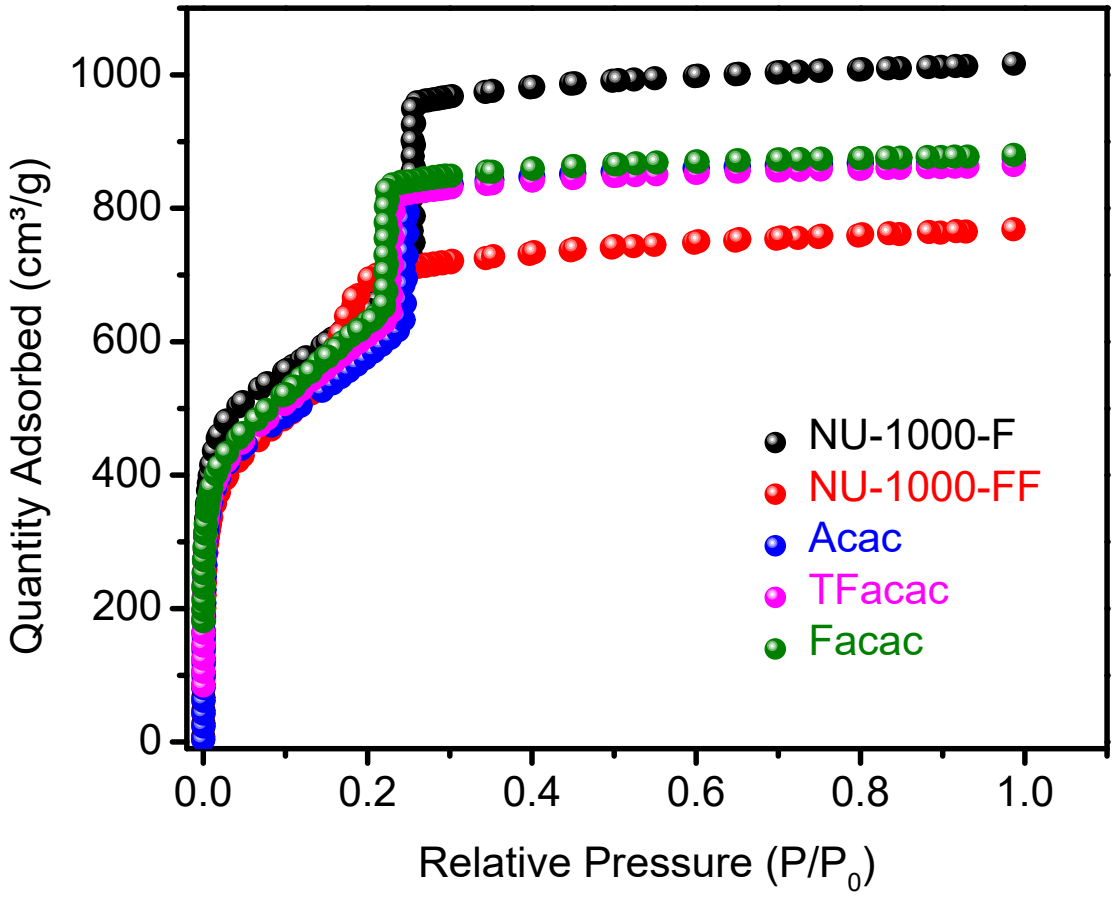

Figure S12. N_2 isotherms of NU-1000-F, NU-1000-FF, Acac-NU-1000, TFacac-NU-1000, and Facac-NU-1000.

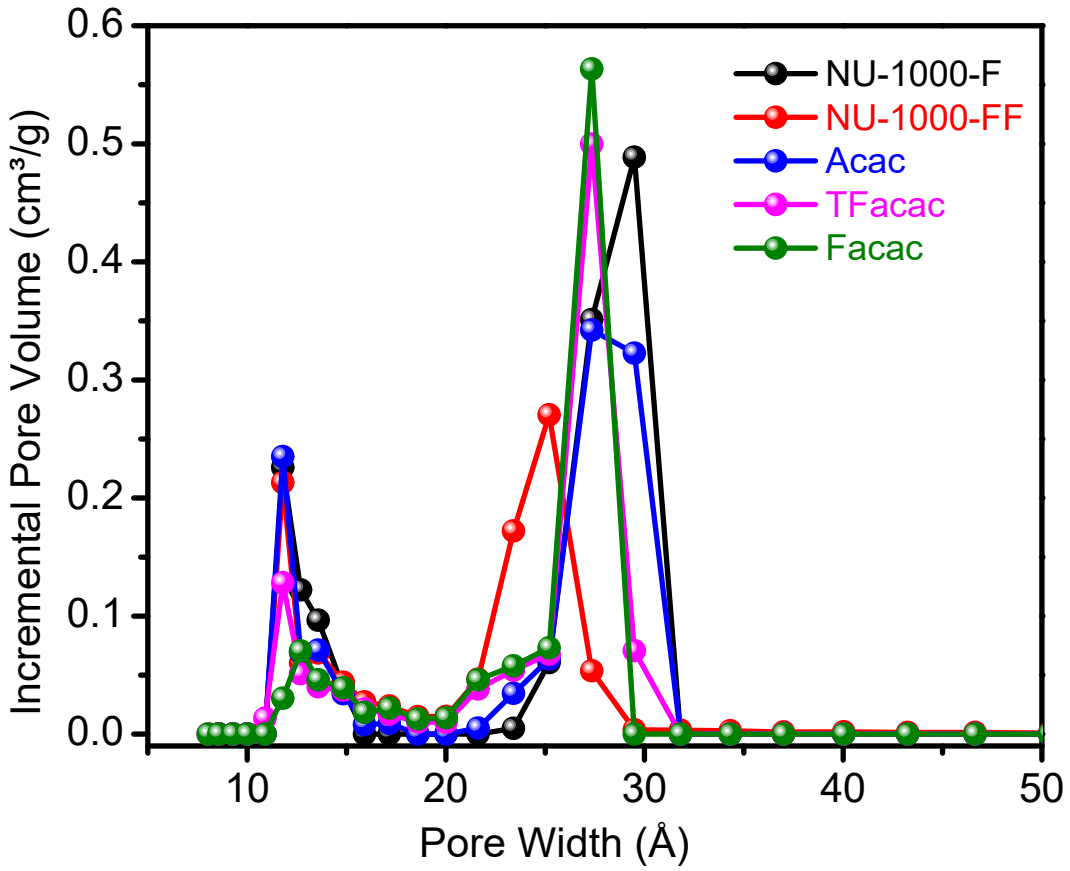

Figure S13. Pore-size distributions of NU-1000-F, NU-1000-FF, Acac-NU-1000, TFacac-NU-1000, and Facac-NU-1000, obtained by NL-DFT (non-local density functional theory) analyses of the N_2 isotherms.

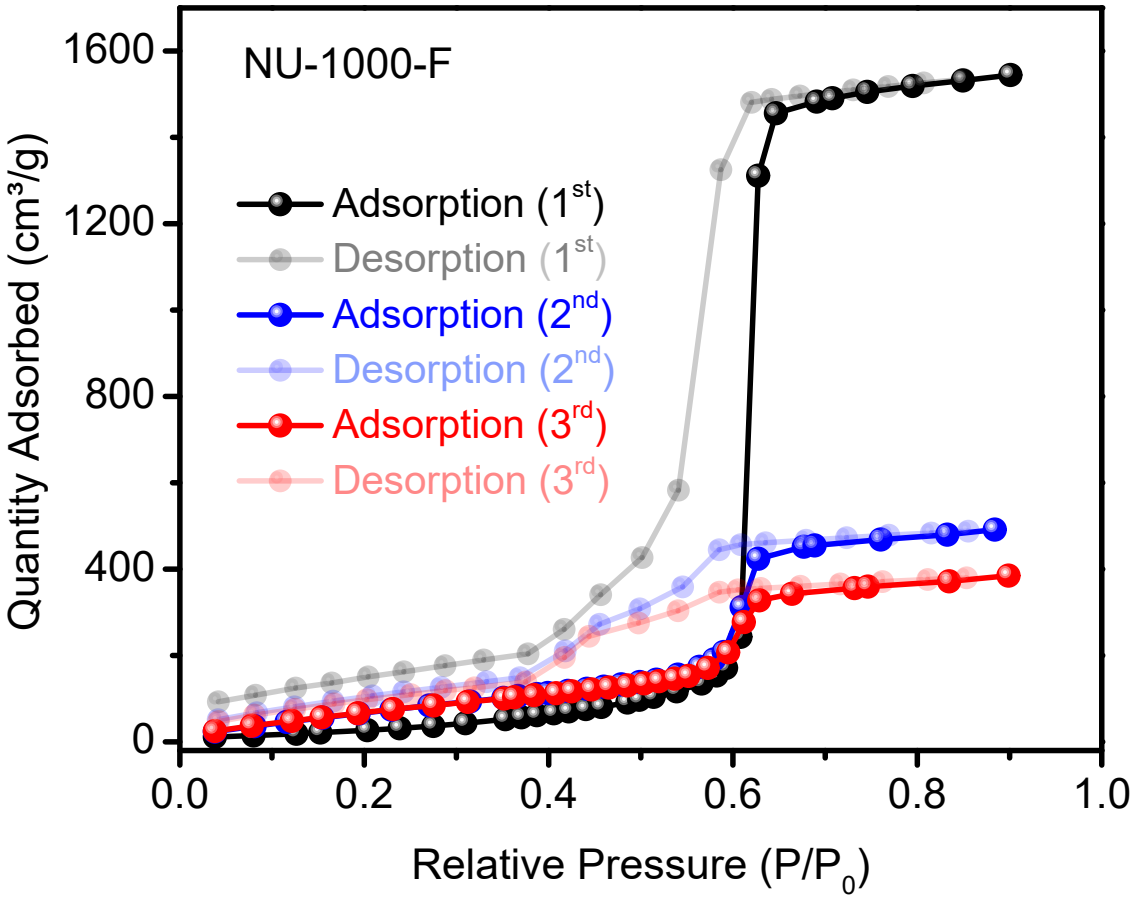

Figure S14. Water vapor isotherm of NU-1000-F for four consecutive adsorption-desorption cycles measured at 14 °C.

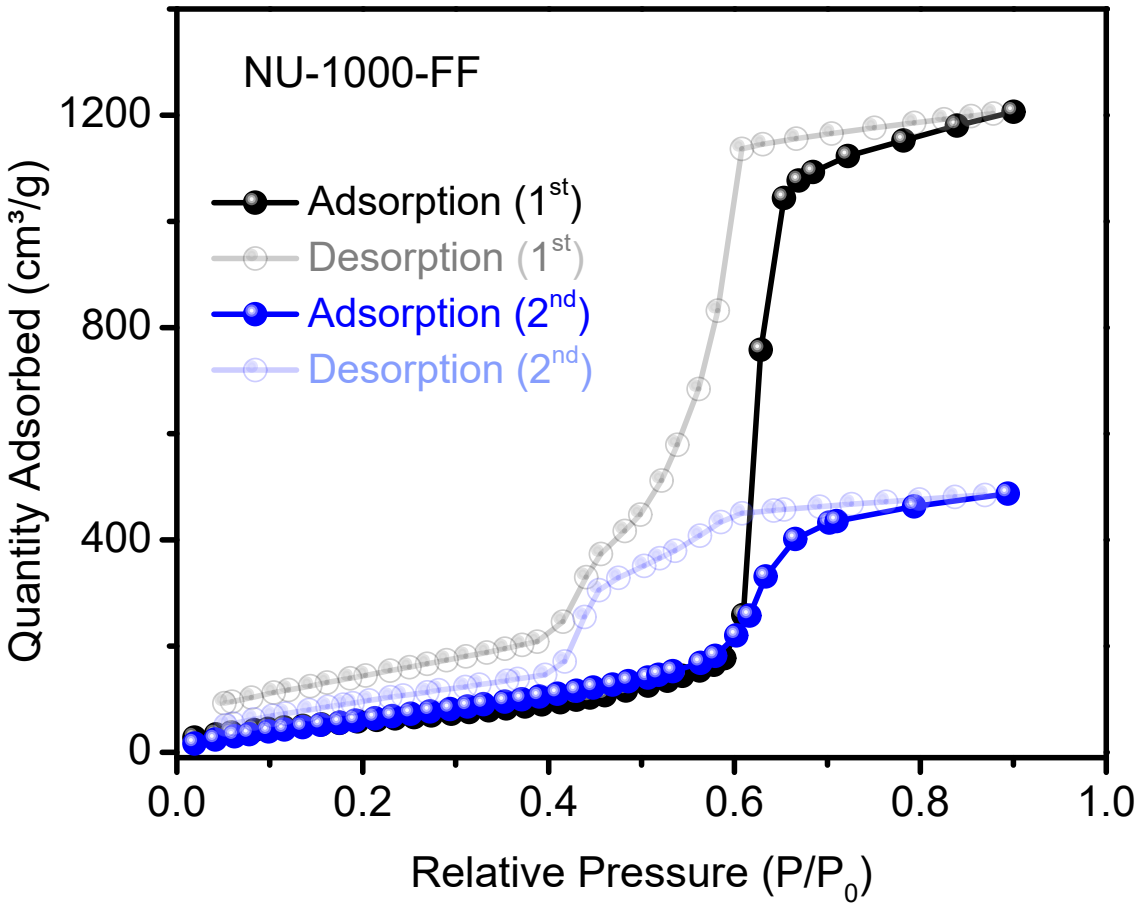

Figure S15. Water vapor isotherm of NU-1000-FF for two consecutive adsorption-desorption cycles measured at 14 °C.

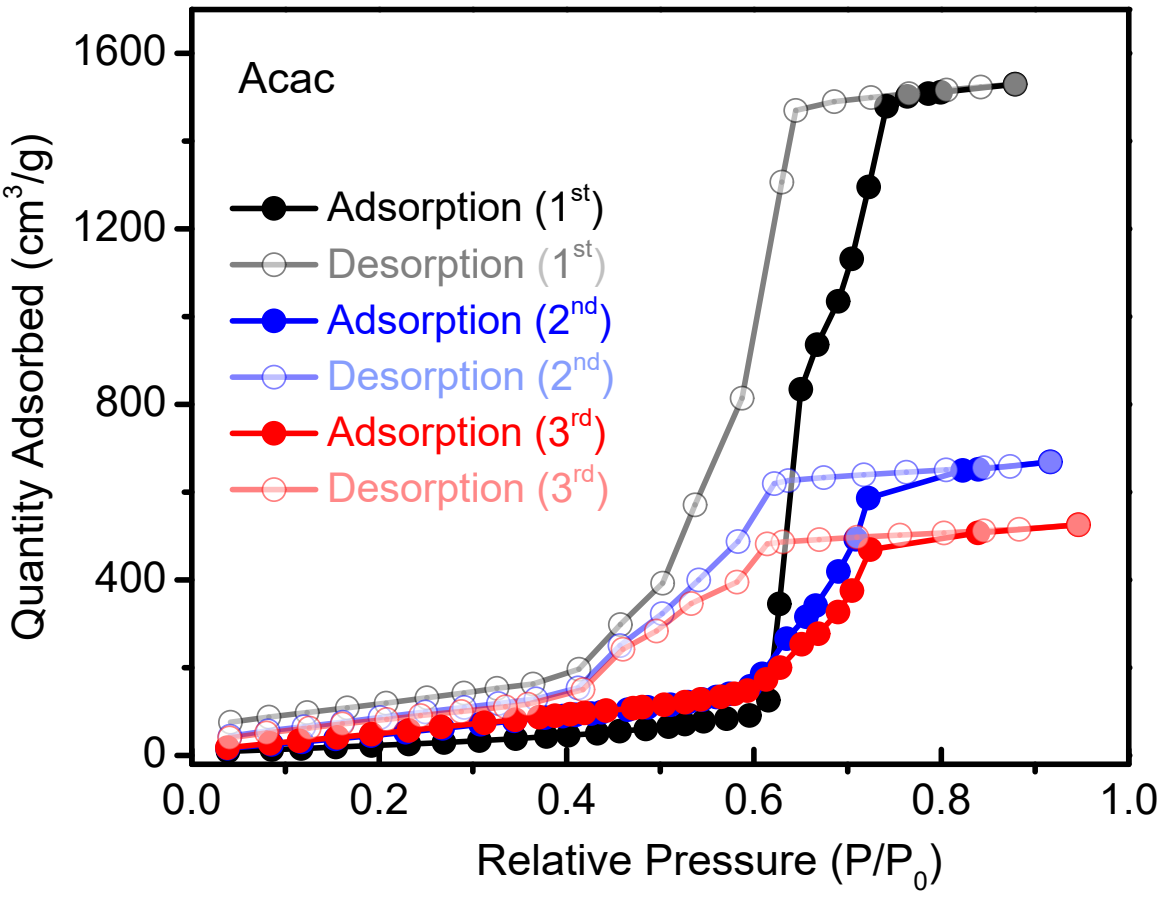

Figure S16. Water vapor isotherm of Acac-NU-1000 for three consecutive adsorption-desorption cycles measured at 14 °C.

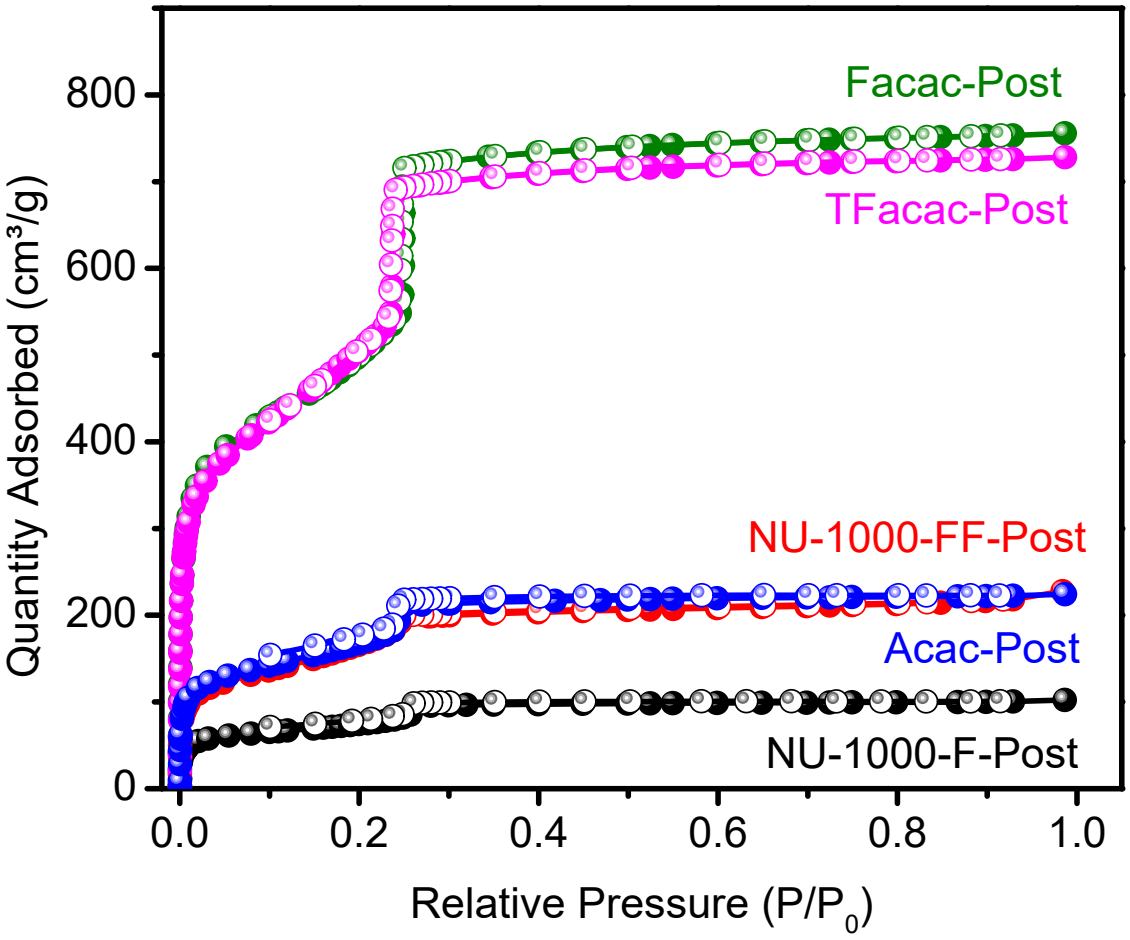

Figure S17. N_2 isotherms of NU-1000-F, NU-1000-FF, Acac-NU-1000, TFacac-NU-1000, and Facac-NU-1000 after water sorption isotherms.

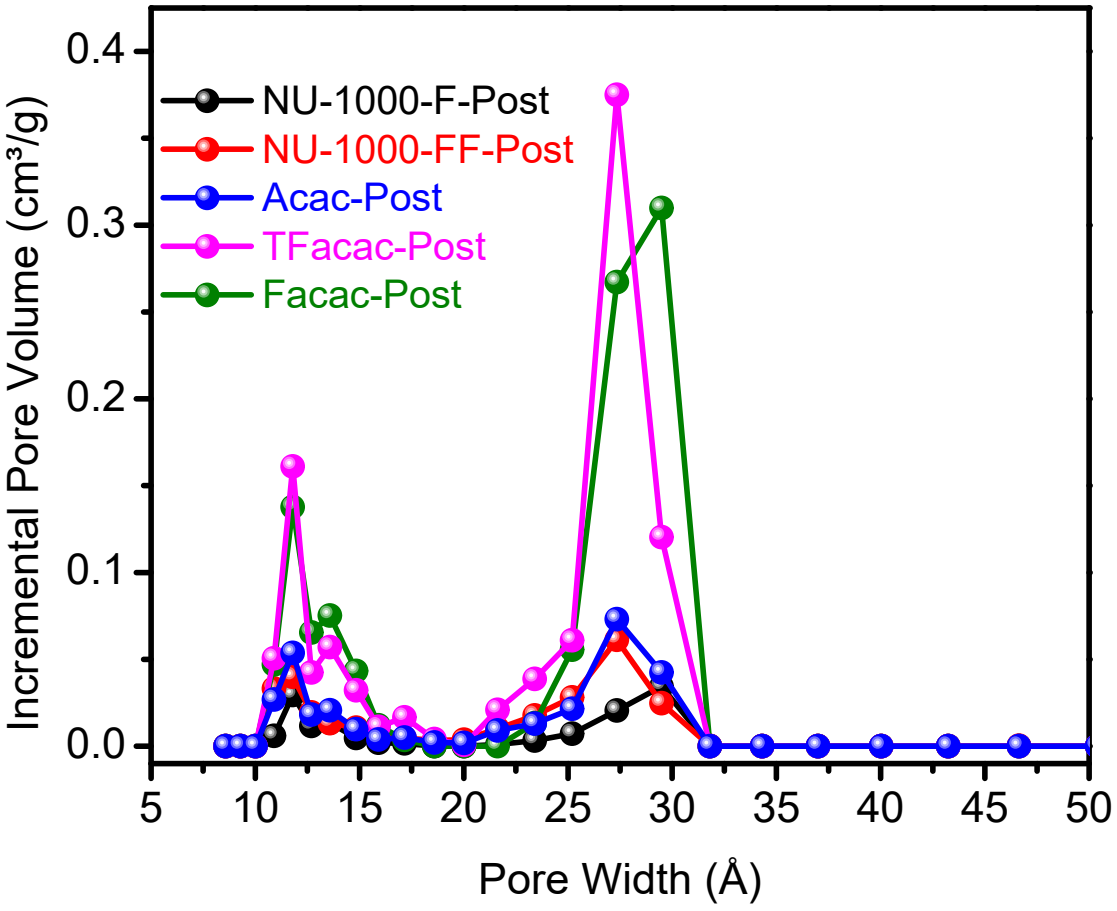

Figure S18. Pore-size distributions of NU-1000-F, NU-1000-FF, Acac-NU-1000, TFacac-NU-1000, and Facac-NU-1000, after water sorption isotherms obtained by NL-DFT (non-local density functional theory) analyses of the N_2 isotherms.

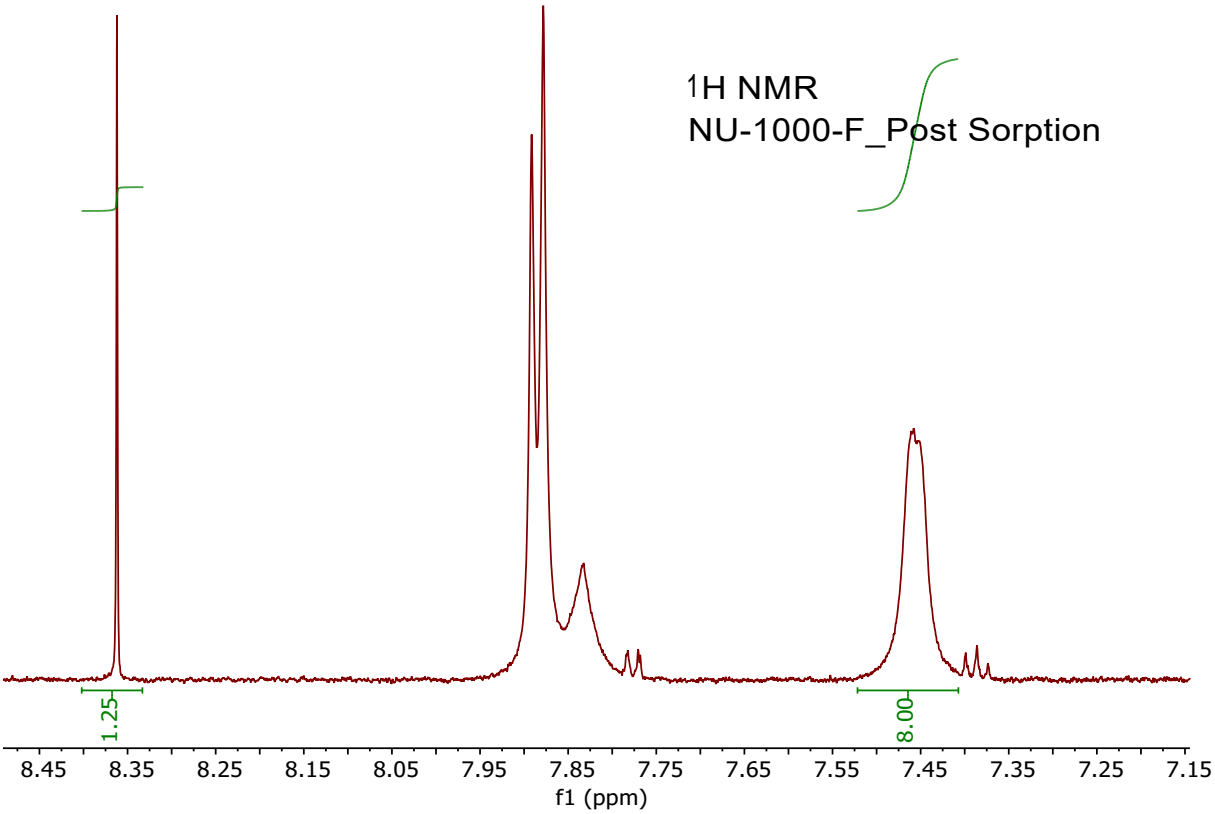

Figure S19. ^{1}H NMR (base digestion) of NU-1000-F after three water adsorption-desorption cycles.

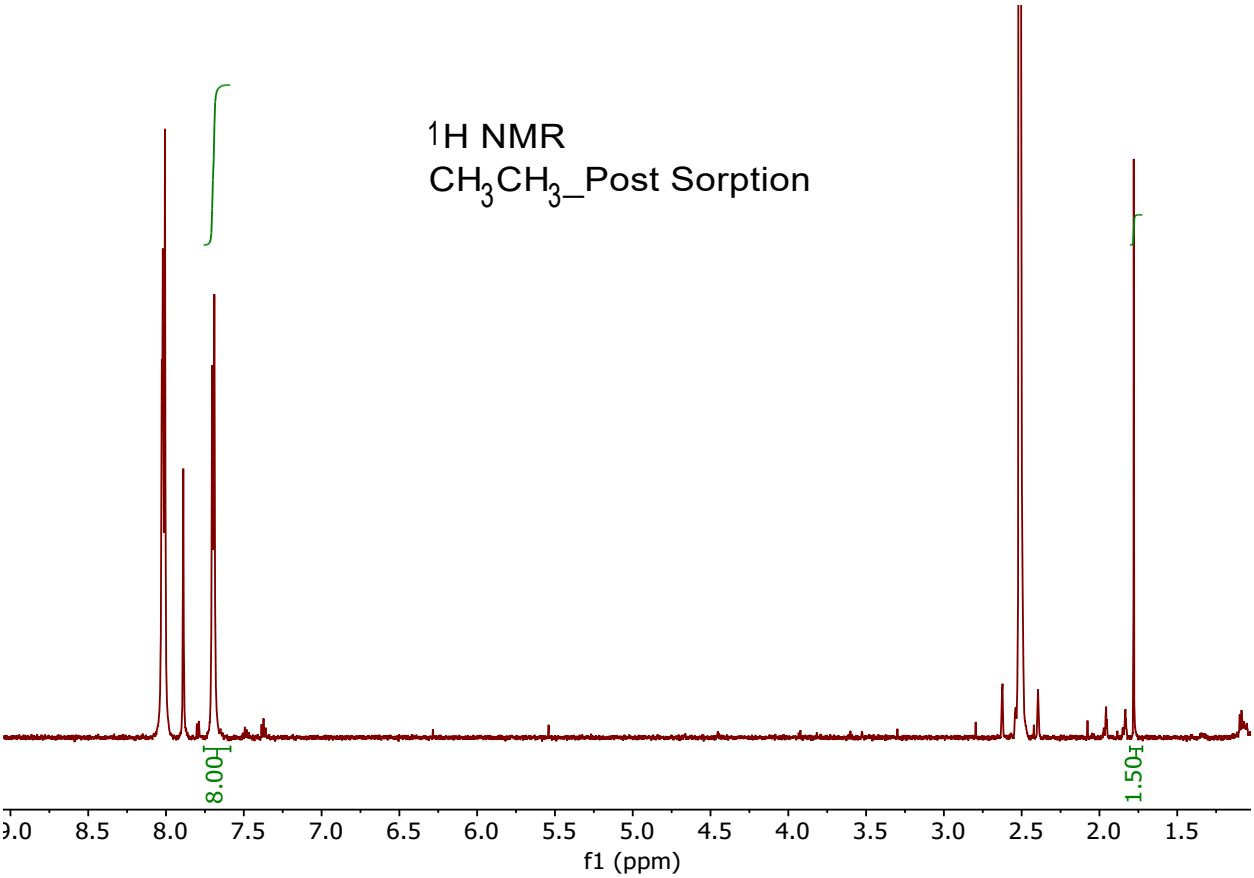

Figure S20. ^{1}H NMR (acid digestion) of Acac-NU-1000 after three water adsorption-desorption cycles.

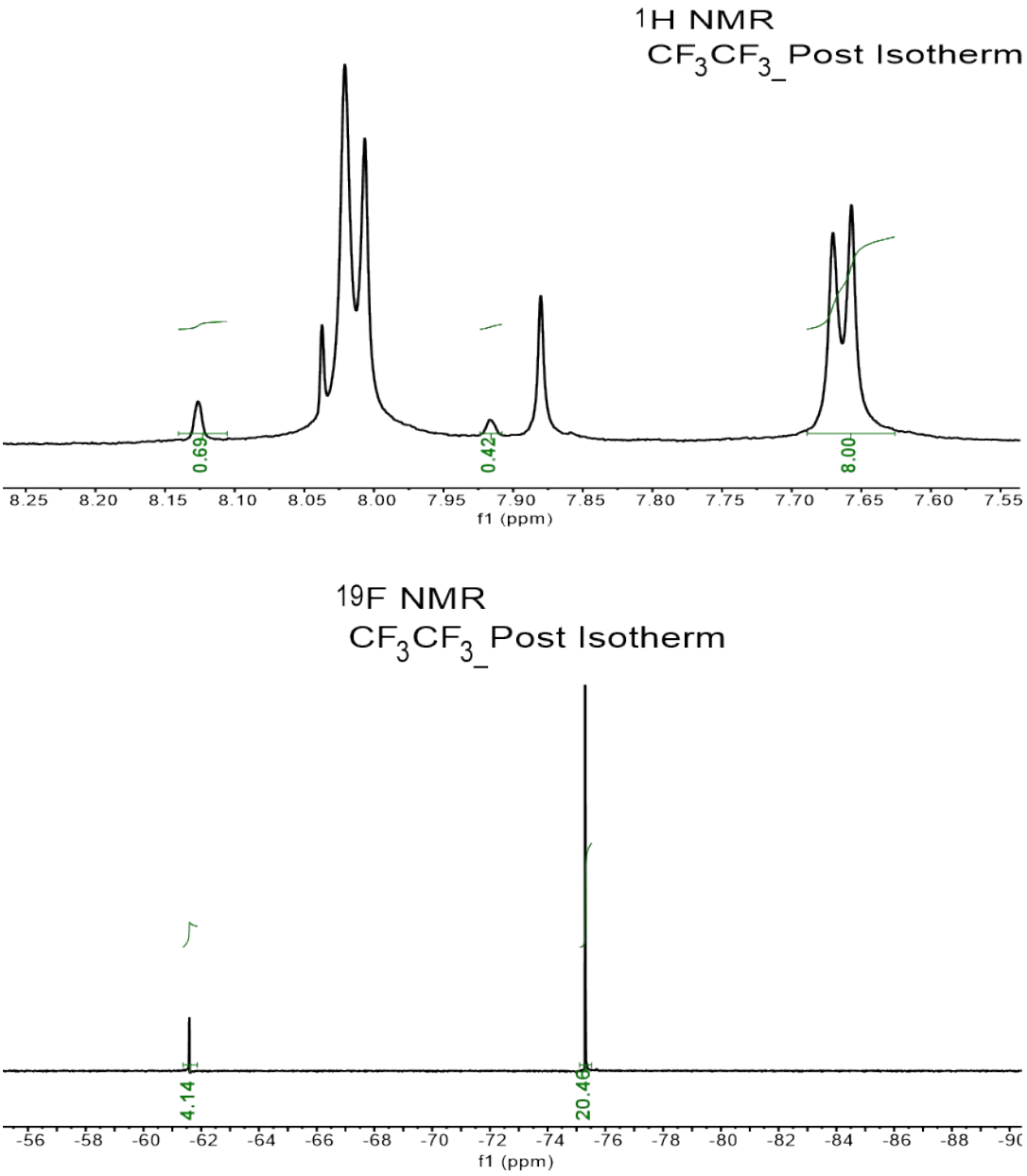

Figure S21. ^{1}H-NMR (acid digestion) and ^{19}F NMR of Facac-NU-1000 after 20 water sorption isotherms.

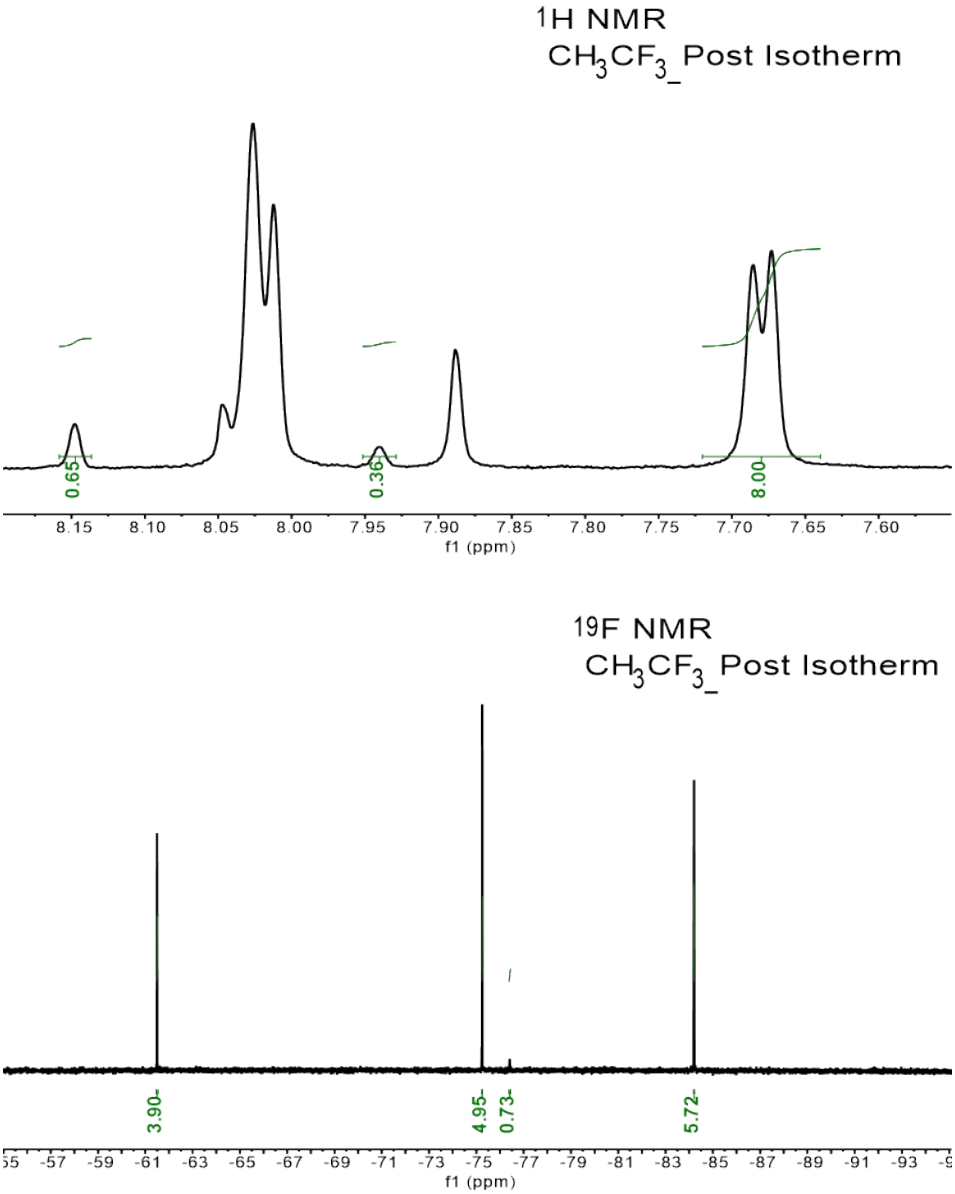

Figure S22. ^{1}H-NMR (acid digestion) and ^{19}F NMR of TFacac-NU-1000 after 20 water sorption isotherms.

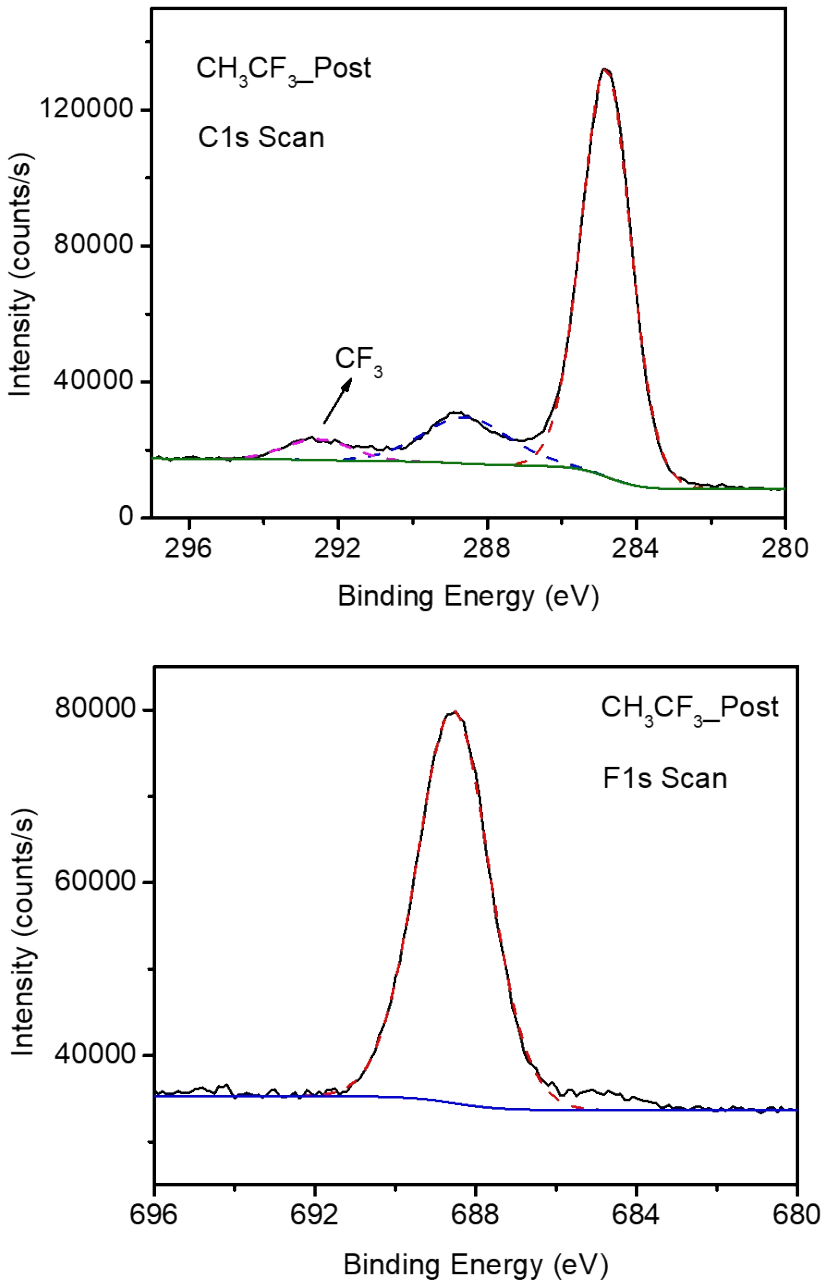

Figure S23. XPS spectra of C1s scan and F1s scan of TFacac-NU-1000 after 20 water sorption cycles.

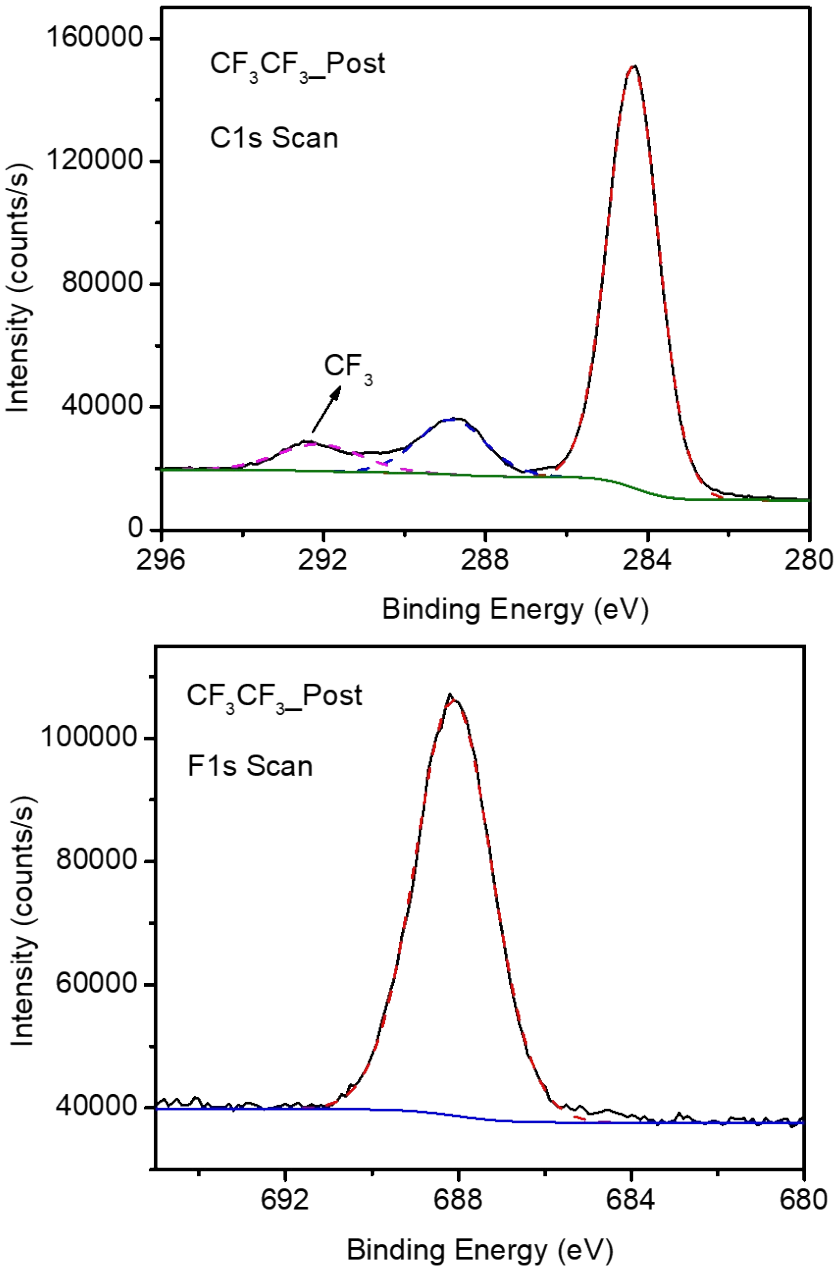

Figure S24. XPS spectra of C1s scan and F1s scan of Facac-NU-1000 after 20 water sorption cycles.

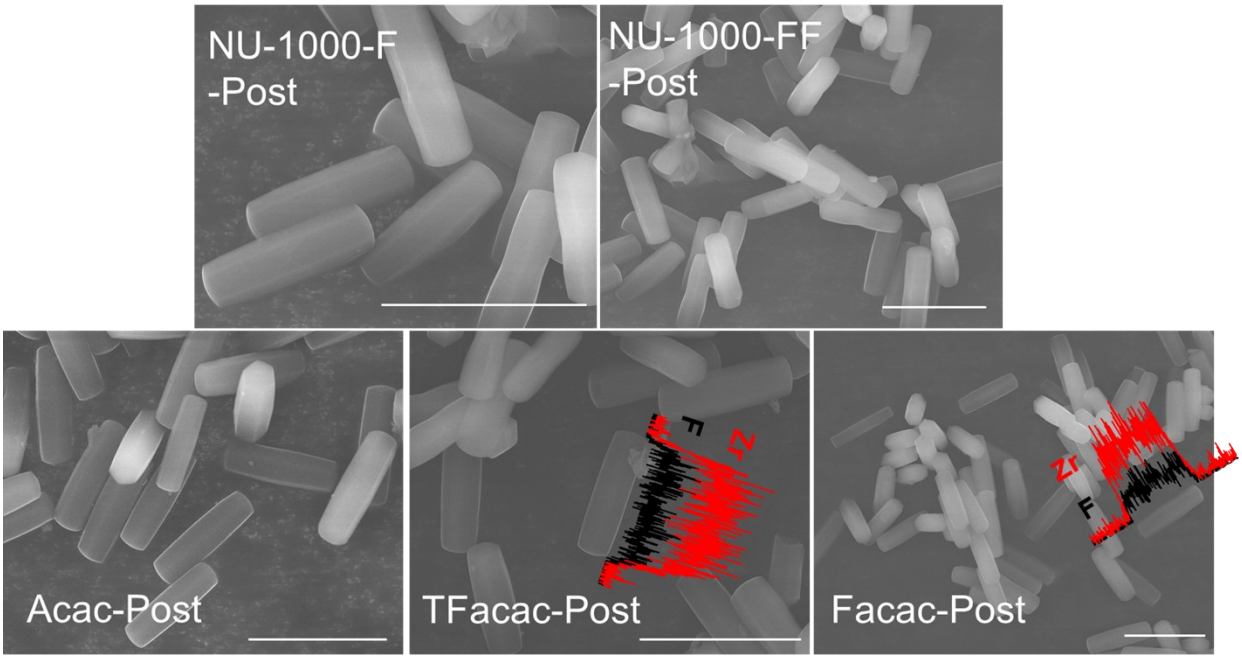

Figure S25. SEM image of NU-1000-F, NU-1000-FF, Acac-NU-1000, TFacac-NU-1000, and Facac-NU-1000 with Zr and F EDS line scans after water isotherms, showing uniform distribution of F throughout the crystals. The scale bar in each image is 10 μm.

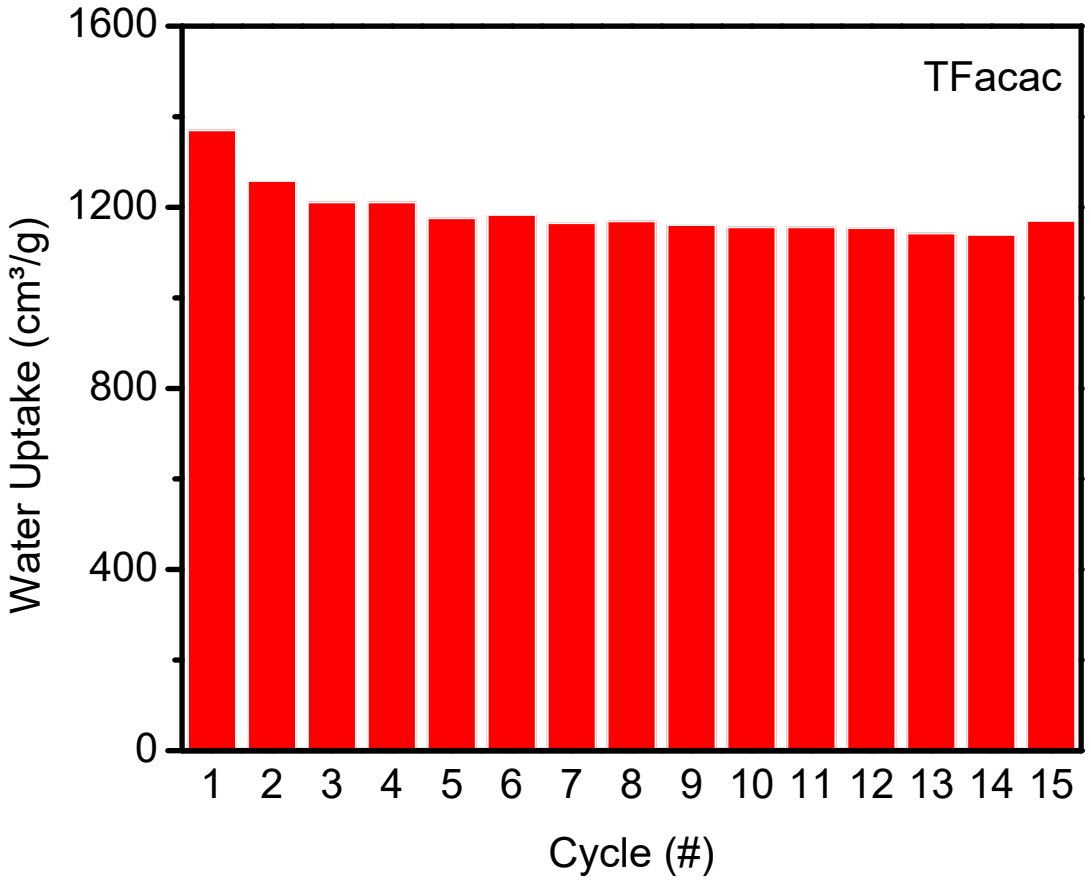

Figure S26. The cycling test of TFacac-NU-1000, showing 15 cycles of water uptake with pressure swing between 20% RH (P/P_0 = 0.20) and 85% RH (P/P_0 = 0.85). Measurements were done at 298 K.

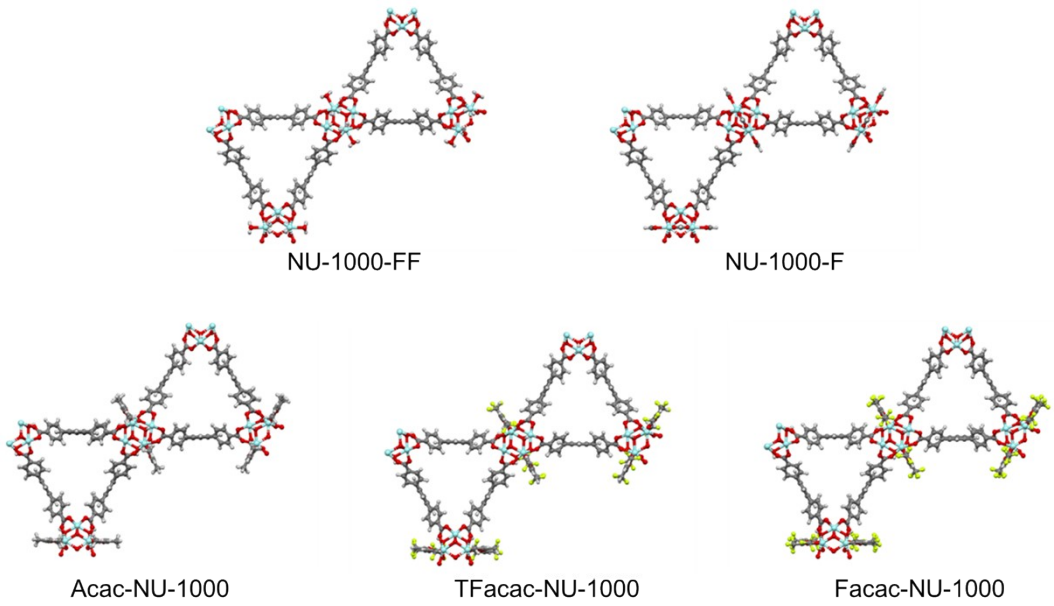

Figure S27. Computational models of NU-1000-FF, NU-1000-F, Acac-NU-1000, TFacac-NU-1000 and Facac-NU-1000. Color: red, oxygen; black, carbon; white, hydrogen; green, fluorine; cyan, zirconium.

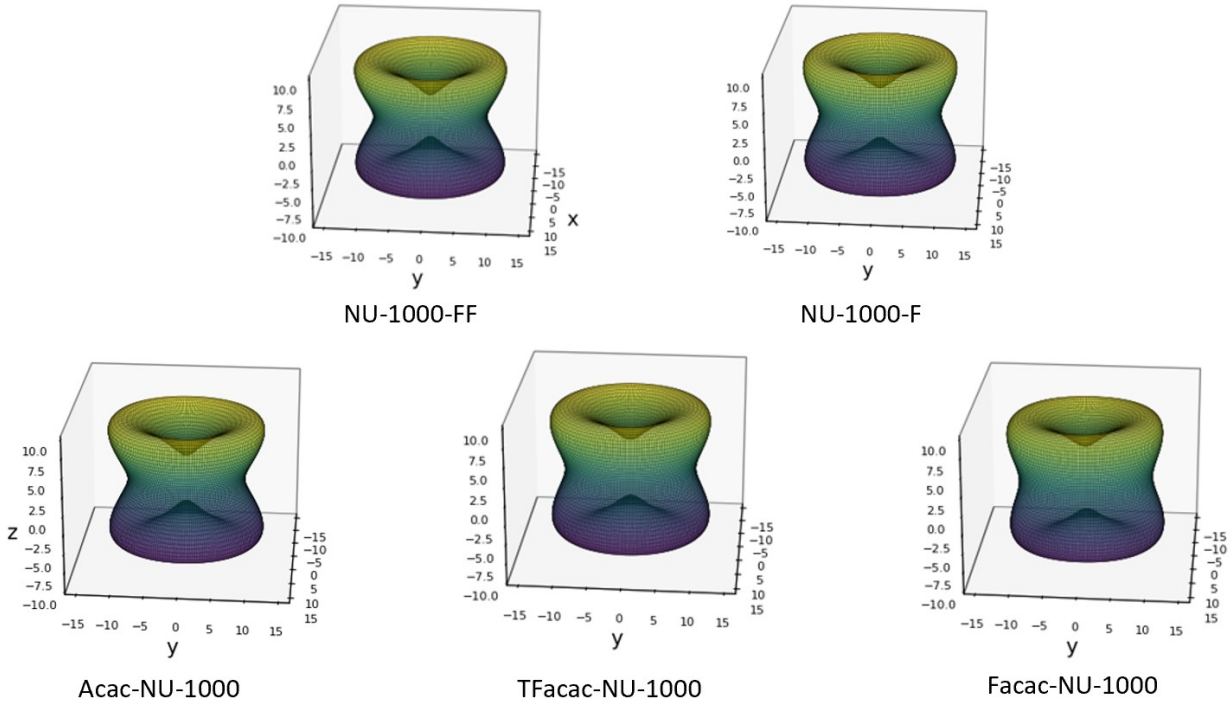

Figure S28. Directional Young's modulus of NU-1000 variants having 0% water loading without intraframework electrostatic interactions being included.

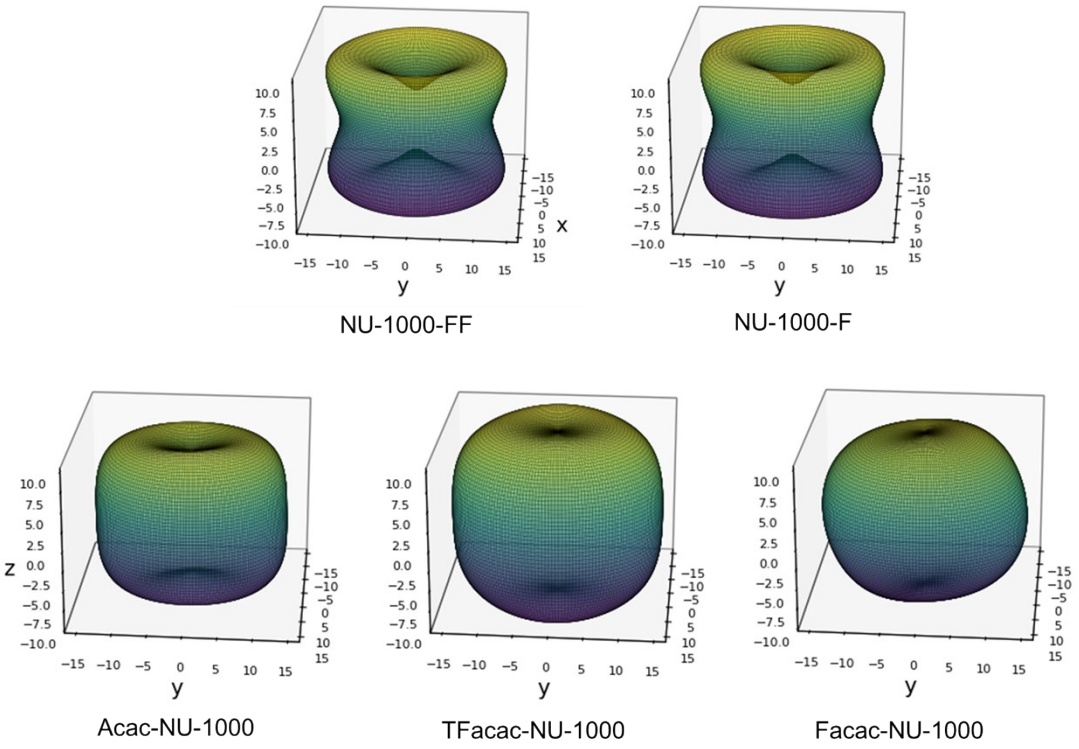

Figure S29. Directional Young's modulus of NU-1000 variants having 0% water loading with intraframework electrostatic interactions being included.

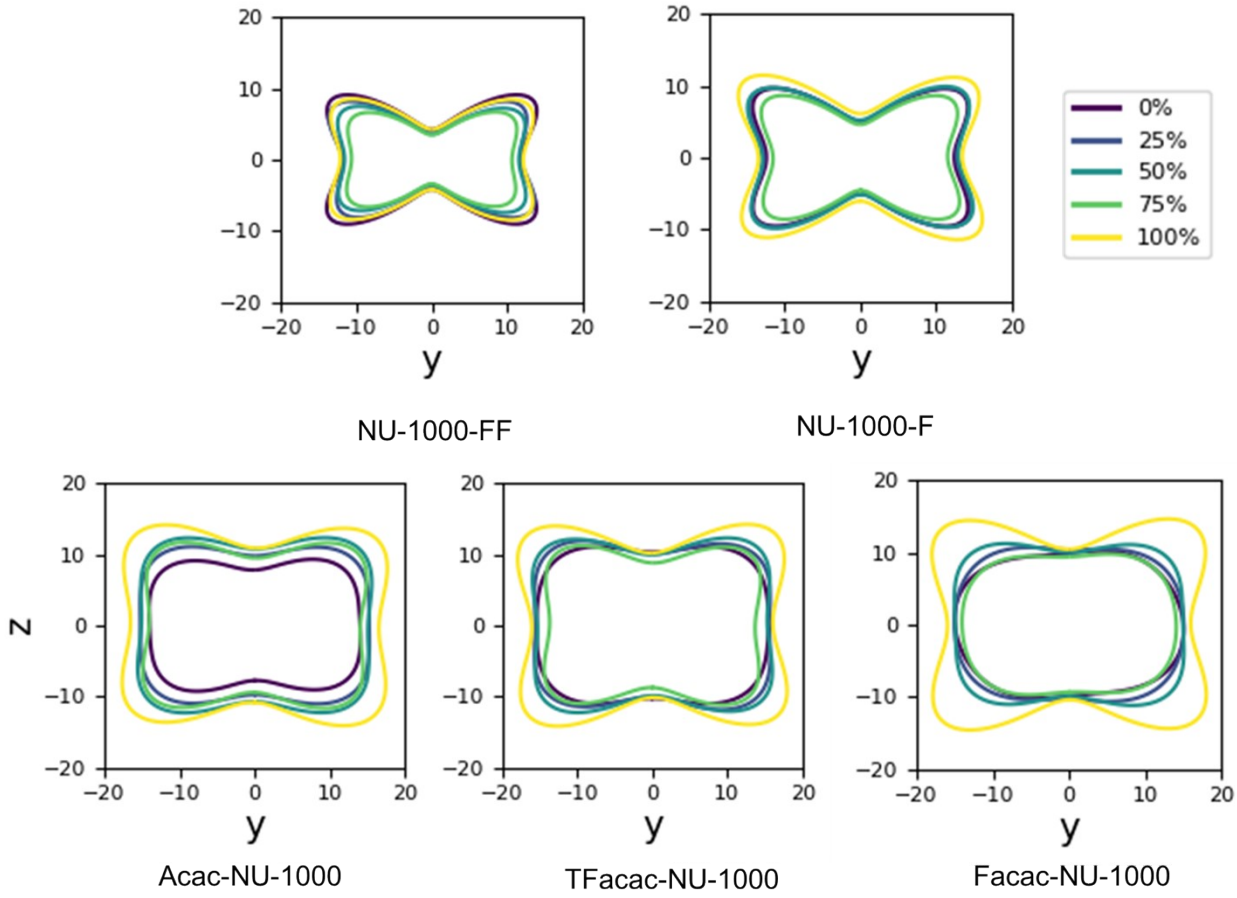

Figure S30. The directional Young's moduli in the yz-plane for five variants of NU-1000 materials with different water loadings (according to the legend). The radius of the contour is the Young's modulus for the corresponding yz-direction.

NU-1000-FF

```
[28.63   9.57 16.71 -0.01 -0.11  0.05]
[ 9.57 28.64 16.64  0.01  0.05  0.04]
[16.71 16.64 18.77 -0.   -0.04  0.04]
[-0.01  0.01 -0.    4.72  0.01  0.08]
[-0.11  0.05 -0.04  0.01  4.73  0.01]
[ 0.05  0.04  0.04  0.08  0.01  9.61]
```

NU-1000-F

```
[27.2   9.97 16.49 -0.04  0.04  0.01]
[ 9.97 27.61 16.63 -0.03  0.03  0.01]
[16.49 16.63 19.68 -0.04  0.03  0.  ]
[-0.04 -0.03 -0.04  5.05 -0.01 -0.  ]
[ 0.04  0.03  0.03 -0.01  5.08  0.01]
[ 0.01  0.01  0.   -0.    0.01  8.92]
```

Acac-NU-1000

```
[26.13  8.85 16.85  0.02  0.08  0.04]
[ 8.85 26.46 16.82 -0.01  0.07  0.01]
[16.85 16.82 23.95  0.09  0.41  0.07]
[ 0.02 -0.01  0.09  4.3   0.03 -0.01]
[ 0.08  0.07  0.41  0.03  4.35  0.03]
[ 0.04  0.01  0.07 -0.01  0.03  8.85]
```

TFacac-NU-1000

```
[26.28  8.86 16.98 -0.02 -0.18  0.02]
[ 8.86 26.49 16.98  0.02  0.13  0.03]
[16.98 16.98 26.67 -0.01 -0.14  0.02]
[-0.02  0.02 -0.01  5.03  0.01  0.14]
[-0.18  0.13 -0.14  0.01  5.02  0.  ]
[ 0.02  0.03  0.02  0.14  0.    8.91]
```

Facac-NU-1000

```
[25.99  8.67 16.93 -0.19  0.1  -0.02]
[ 8.67 26.09 16.85 -0.05 -0.02 -0.06]
[16.93 16.85 26.34  0.12 -0.04 -0.06]
[-0.19 -0.05  0.12  4.08 -0.04 -0.08]
[ 0.1  -0.02 -0.04 -0.04  4.08 -0.01]
[-0.02 -0.06 -0.06 -0.08 -0.01  8.81]
```

Figure S31. Average elastic tensor matrices calculated for different NU-1000 variants from molecular simulations at 0% water loadings.

NU-1000-FF

```
[28.71  9.74 16.07 -0.1   0.01  0.12]
[ 9.74 28.72 16.19 -0.26 -0.19 -0.01]
[16.07 16.19 17.52  0.01 -0.11 -0.01]
[-0.1  -0.26  0.01  4.14 -0.01 -0.12]
[ 0.01 -0.19 -0.11 -0.01  4.25 -0.06]
[ 0.12 -0.01 -0.01 -0.12 -0.06  9.62]
```

NU-1000-F

```
[26.25 10.23 15.64 -0.09 -0.03 -0.05]
[10.23 26.98 15.82 -0.14  0.11  0.05]
[15.64 15.82 18.5  -0.07 -0.04  0.01]
[-0.09 -0.14 -0.07  5.29  0.07 -0.05]
[-0.03  0.11 -0.04  0.07  4.95  0.09]
[-0.05  0.05  0.01 -0.05  0.09  8.54]
```

Acac-NU-1000

```
[26.32  9.   16.93 -0.07 -0.03 -0.07]
[ 9.   26.39 16.81 -0.07 -0.03 -0.06]
[16.93 16.81 25.89 -0.07  0.15 -0.01]
[-0.07 -0.07 -0.07  5.2   0.   -0.04]
[-0.03 -0.03  0.15  0.    5.2  -0.02]
[-0.07 -0.06 -0.01 -0.04 -0.02  8.83]
```

TFacac-NU-1000

```
[26.44  8.99 16.87  0.06 -0.09 -0.02]
[ 8.99 26.82 16.95 -0.09  0.2  -0.04]
[16.87 16.95 26.14 -0.13 -0.03  0.08]
[ 0.06 -0.09 -0.13  5.6   0.04  0.1 ]
[-0.09  0.2  -0.03  0.04  5.49  0.05]
[-0.02 -0.04  0.08  0.1   0.05  8.89]
```

Facac-NU-1000

```
[26.    8.74 16.94  0.03 -0.03 -0.19]
[ 8.74 25.95 16.95 -0.08 -0.12 -0.15]
[16.94 16.95 26.94 -0.09 -0.01  0.02]
[ 0.03 -0.08 -0.09  4.51 -0.03  0.01]
[-0.03 -0.12 -0.01 -0.03  4.53 -0.05]
[-0.19 -0.15  0.02  0.01 -0.05  8.74]
```

Figure S32. Average elastic tensor matrices calculated for different NU-1000 variants from molecular simulations at 25% water loadings.

NU-1000-FF

```
[28.2   9.79 15.76  0.09  0.15 -0.03]
[ 9.79 28.78 15.81 -0.13  0.03 -0.05]
[15.76 15.81 16.55 -0.08 -0.   -0.05]
[ 0.09 -0.13 -0.08  3.67 -0.01 -0.06]
[ 0.15  0.03 -0.   -0.01  3.58 -0.04]
[-0.03 -0.05 -0.05 -0.06 -0.04  9.63]
```

NU-1000-F

```
[26.48  9.81 15.56 -0.08 -0.07  0.21]
[ 9.81 26.32 15.16 -0.1   0.05  0.01]
[15.56 15.16 18.24  0.09 -0.09  0.14]
[-0.08 -0.1   0.09  5.39  0.05 -0.03]
[-0.07  0.05 -0.09  0.05  5.21  0.01]
[ 0.21  0.01  0.14 -0.03  0.01  8.35]
```

Acac-NU-1000

```
[26.18  9.   17.3   0.09 -0.01 -0.07]
[ 9.   26.08 17.33  0.19 -0.09  0.02]
[17.3  17.33 27.82  0.09  0.11 -0.  ]
[ 0.09  0.19  0.09  5.84 -0.1   0.02]
[-0.01 -0.09  0.11 -0.1   5.6   0.05]
[-0.07  0.02 -0.    0.02  0.05  8.71]
```

TFacac-NU-1000

```
[26.53  9.11 17.04  0.01 -0.13  0.06]
[ 9.11 26.74 17.15 -0.07  0.07 -0.05]
[17.04 17.15 26.29  0.07  0.03 -0.02]
[ 0.01 -0.07  0.07  6.03  0.03  0.08]
[-0.13  0.07  0.03  0.03  6.   -0.03]
[ 0.06 -0.05 -0.02  0.08 -0.03  8.8 ]
```

Facac-NU-1000

```
[25.98  8.94 17.28 -0.09 -0.05  0.  ]
[ 8.94 26.4  17.37 -0.18 -0.17 -0.05]
[17.28 17.37 27.07 -0.14  0.02 -0.09]
[-0.09 -0.18 -0.14  5.16  0.11  0.08]
[-0.05 -0.17  0.02  0.11  5.32 -0.09]
[ 0.   -0.05 -0.09  0.08 -0.09  8.72]
```

Figure S33. Average elastic tensor matrices calculated for different NU-1000 variants from molecular simulations at 50% water loadings.

NU-1000-FF

```
[29.09 10.16 17.23  0.1   0.03  0.01]
[10.16 28.74 16.92  0.11 -0.15  0.02]
[17.23 16.92 18.4   0.09  0.09  0.07]
[ 0.1   0.11  0.09  3.19 -0.01 -0.03]
[ 0.03 -0.15  0.09 -0.01  3.37  0.02]
[ 0.01  0.02  0.07 -0.03  0.02  9.58]
```

NU-1000-F

```
[25.02  9.87 15.49 -0.09  0.04 -0.11]
[ 9.87 25.7  15.56 -0.1  -0.05 -0.28]
[15.49 15.56 18.29 -0.04  0.13  0.02]
[-0.09 -0.1  -0.04  4.56 -0.13 -0.07]
[ 0.04 -0.05  0.13 -0.13  4.72  0.05]
[-0.11 -0.28  0.02 -0.07  0.05  8.13]
```

Acac-NU-1000

```
[23.81  8.66 16.77  0.25 -0.12  0.12]
[ 8.66 25.45 17.24  0.24 -0.06 -0.07]
[16.77 17.24 26.85  0.15 -0.18 -0.04]
[ 0.25  0.24  0.15  5.65  0.06 -0.  ]
[-0.12 -0.06 -0.18  0.06  5.81  0.03]
[ 0.12 -0.07 -0.04 -0.    0.03  8.44]
```

TFacac-NU-1000

```
[24.21  8.41 16.81 -0.24 -0.05  0.14]
[ 8.41 25.35 17.07 -0.06  0.1  -0.06]
[16.81 17.07 26.08 -0.24  0.06  0.11]
[-0.24 -0.06 -0.24  5.4  -0.06  0.1 ]
[-0.05  0.1   0.06 -0.06  5.27 -0.02]
[ 0.14 -0.06  0.11  0.1  -0.02  8.43]
```

Facac-NU-1000

```
[24.53  8.56 16.85  0.01  0.02 -0.13]
[ 8.56 25.37 17.03  0.04 -0.05 -0.13]
[16.85 17.03 26.53  0.12 -0.28 -0.06]
[ 0.01  0.04  0.12  4.11  0.02  0.09]
[ 0.02 -0.05 -0.28  0.02  4.26 -0.02]
[-0.13 -0.13 -0.06  0.09 -0.02  8.51]
```

Figure S34. Average elastic tensor matrices calculated for different NU-1000 variants from molecular simulations at 75% water loadings.

NU-1000-FF

```
[30.45 12.01 18.76 -0.05  0.    0.16]
[12.01 30.81 18.65 -0.04 -0.07  0.12]
[18.76 18.65 20.67 -0.08 -0.08  0.13]
[-0.05 -0.04 -0.08  4.28  0.03 -0.15]
[ 0.   -0.07 -0.08  0.03  4.17  0.03]
[ 0.16  0.12  0.13 -0.15  0.03  9.4 ]
```

NU-1000-F

```
[29.7  13.04 19.37  0.14 -0.01  0.1 ]
[13.04 30.04 19.45 -0.13  0.   -0.05]
[19.37 19.45 23.66 -0.01 -0.13  0.04]
[ 0.14 -0.13 -0.01  6.18  0.15 -0.11]
[-0.01  0.   -0.13  0.15  6.06  0.02]
[ 0.1  -0.05  0.04 -0.11  0.02  8.89]
```

Acac-NU-1000

```
[29.86 12.2  20.36  0.11 -0.01  0.04]
[12.2  30.29 20.41  0.03 -0.01 -0.15]
[20.36 20.41 30.54 -0.12 -0.06  0.04]
[ 0.11  0.03 -0.12  7.05  0.1   0.07]
[-0.01 -0.01 -0.06  0.1   7.05 -0.05]
[ 0.04 -0.15  0.04  0.07 -0.05  9.06]
```

TFacac-NU-1000

```
[30.08 12.23 20.21  0.02 -0.05 -0.19]
[12.23 30.14 20.29 -0.07  0.14 -0.16]
[20.21 20.29 29.56  0.12  0.21 -0.08]
[ 0.02 -0.07  0.12  7.37  0.06 -0.02]
[-0.05  0.14  0.21  0.06  7.34 -0.15]
[-0.19 -0.16 -0.08 -0.02 -0.15  8.95]
```

Facac-NU-1000

```
[29.69 11.98 20.21 -0.12  0.03 -0.12]
[11.98 29.88 20.36 -0.06 -0.15 -0.17]
[20.21 20.36 30.15  0.    0.08 -0.02]
[-0.12 -0.06  0.    7.63  0.    0.03]
[ 0.03 -0.15  0.08  0.    7.8  -0.04]
[-0.12 -0.17 -0.02  0.03 -0.04  9.05]
```

Figure S35. Average elastic tensor matrices calculated for different NU-1000 variants from molecular simulations at 100% water loadings.

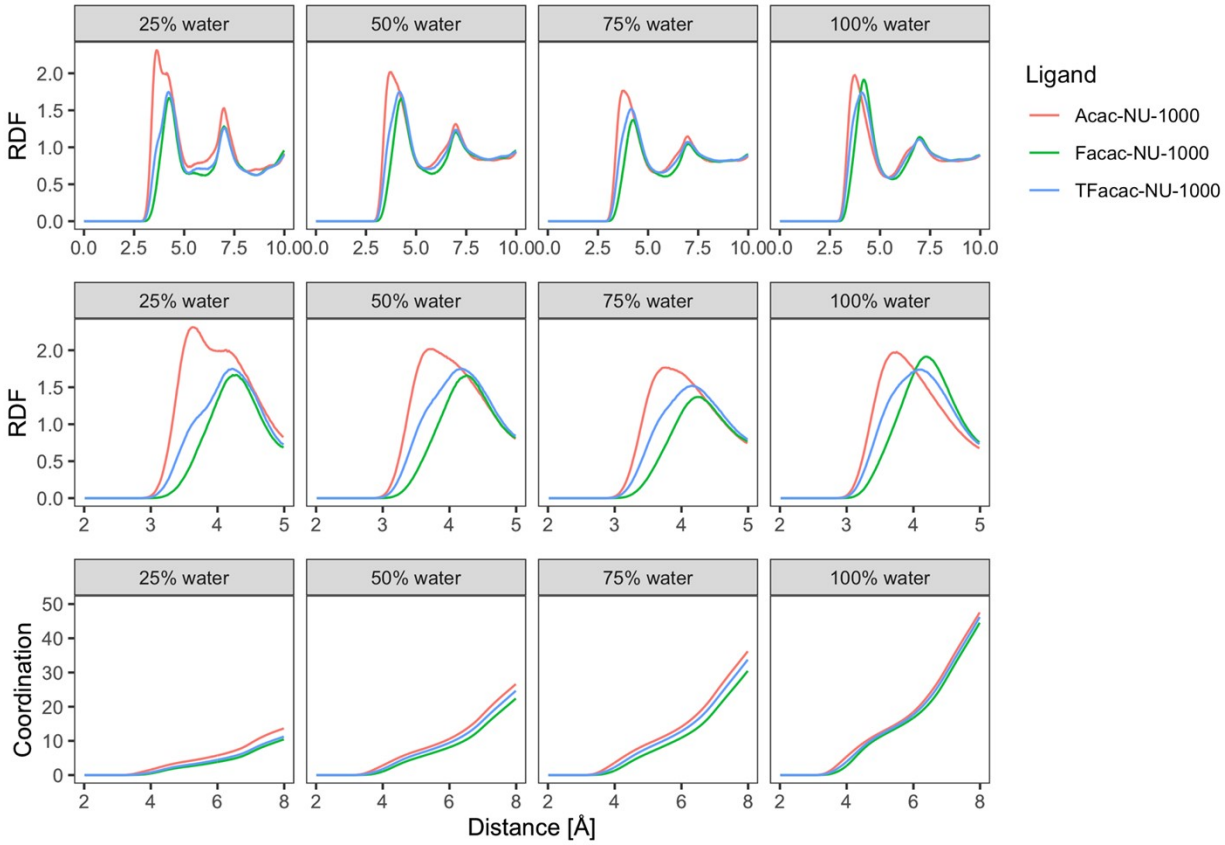

Figure S36. (top) Radial distribution functions of water oxygen and sp^3 carbon (0-10 Å); (middle) zoomed radial distribution functions of water oxygen and sp^3 carbon (2-5 Å); (bottom) coordination plots showing the number of water-carbon pairs within the distance on the x-axis. Red: Acac-NU-1000, cyan: TFacac-NU-1000, and green: Facac-NU-1000.

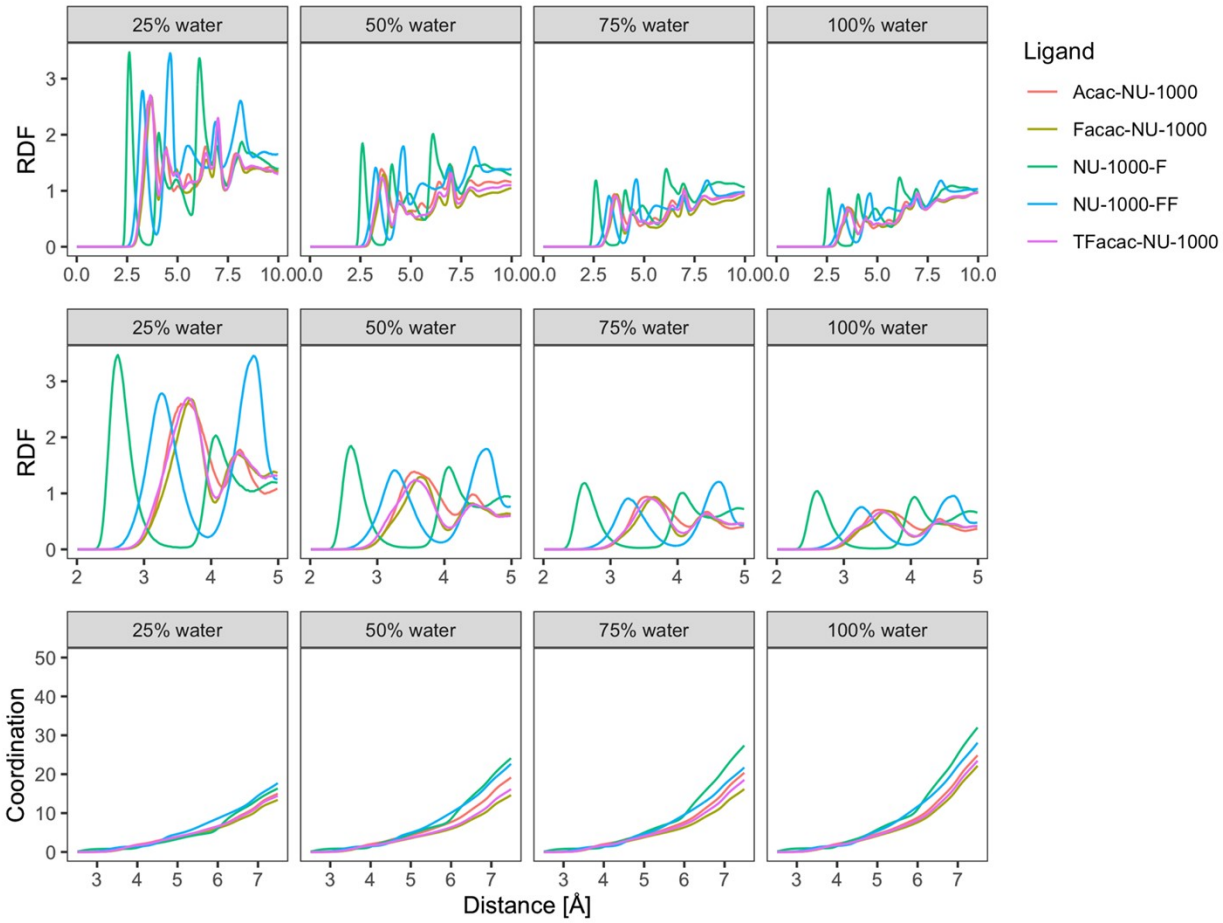

Figure S37. (top) Radial distribution functions of water oxygen and Zr ion (0-10 Å); (middle) Zoomed radial distribution functions of water oxygen and Zr ion (2-5 Å); (bottom) Coordination plots showing the number of water-Zr pairs within the distance on the x-axis. Red: Acac-NU-1000, purple: TFacac-NU-1000, yellow: Facac-NU-1000, green: NU-1000-F, and cyan: NU-1000-FF.

Table S1. Eigenvalues λ_i (i = 1 to 6) of elastic tensor matrix obtained from molecular simulations.

MOF	Water Loading [%]	λ_1	λ_2	λ_3	λ_4	λ_5	λ_6
Acac-NU-1000	0	4.27	4.3	5.17	8.85	17.45	54.01
Acac-NU-1000	25	5.18	5.2	6.32	8.83	17.36	54.95
Acac-NU-1000	50	5.55	5.86	6.74	8.71	17.13	56.23
Acac-NU-1000	75	5.58	5.76	5.91	8.44	15.96	54.36
Acac-NU-1000	100	6.85	7	7.23	9.06	17.88	65.83
Tfacac-NU-1000	0	5.01	5.03	6.57	8.92	17.53	55.35
Tfacac-NU-1000	25	5.47	5.6	6.51	8.9	17.64	55.26
Tfacac-NU-1000	50	5.98	6.02	6.41	8.8	17.53	55.65
Tfacac-NU-1000	75	5.24	5.37	5.46	8.43	16.37	53.86
Tfacac-NU-1000	100	6.57	7.29	7.44	8.97	17.88	65.29
Facac-NU-1000	0	4.03	4.1	6.3	8.81	17.37	54.78
Facac-NU-1000	25	4.49	4.55	6.54	8.75	17.24	55.11
Facac-NU-1000	50	5.1	5.36	6.28	8.72	17.25	55.93
Facac-NU-1000	75	4.1	4.24	5.83	8.51	16.39	54.24
Facac-NU-1000	100	6.66	7.63	7.81	9.06	17.81	65.23
NU-1000-F	0	3.49	5.05	5.08	8.92	17.43	53.56
NU-1000-F	25	3.61	4.94	5.3	8.54	16.38	51.74
NU-1000-F	50	3.7	5.2	5.41	8.35	16.59	50.73
NU-1000-F	75	3.21	4.49	4.79	8.14	15.49	50.3
NU-1000-F	100	4.19	5.96	6.28	8.89	16.83	62.37
NU-1000-FF	0	2.98	4.71	4.73	9.61	19.07	53.99
NU-1000-FF	25	2.87	4.15	4.25	9.62	18.98	53.09
NU-1000-FF	50	2.58	3.58	3.67	9.63	18.7	52.24
NU-1000-FF	75	2.45	3.19	3.39	9.58	18.75	55.01
NU-1000-FF	100	3.01	4.16	4.29	9.4	18.62	60.3

References

1. T. C. Wang, N. A. Vermeulen, I. S. Kim, A. B. Martinson, J. F. Stoddart, J. T. Hupp, O. K. Farha, *Nat. Protoc.* **2016,** *11*, 149.
2. Z. Wang, K. M. Schmalbach, R. L. Combs, Y. Chen, R. L. Penn, N. A. Mara, A. Stein, *ACS Appl. Mater. Interfaces* **2020,** *12*, 49971.
3. R. Anderson, D. A. Gómez-Gualdrón, *CrystEngComm* **2019,** *21*, 1653.
4. E. Argueta, J. Shaji, A. Gopalan, P. Liao, R. Q. Snurr, D. A. Gomez-Gualdron, *J. Chem. Theory Comput.* **2018,** *14*, 365.
5. D. Dubbeldam, S. Calero, D. E. Ellis, R. Q. Snurr, *Mol. Simul.* **2015,** *42*, 81.
6. D. M. Eike, E. J. Maginn, *J. Chem. Phys.* **2006,** *124*, 164503.